Electronic Supplementary Material (ESI) for Organic & Biomolecular Chemistry.

Supplementary Information

Synthesis and characterization of bent fluorine-containing donor-π-acceptor molecules as intense luminophores with large Stokes shifts

Shigeyuki Yamada,*[,a] Akito Nishizawa,[a] Masato Morita,[a] Takuya Hosokai,[b] Yusuke Okabayashi,[b] Tomohiro Agou,[c] Takaaki Hosoya,[c] Toshio Kubota [c] and Tsutomu Konno [a]

[a] Faculty of Molecular Chemistry and Engineering, Kyoto Institute of Technology, Matsugasaki, Sakyo-ku, Kyoto 606-8585, Japan; Tel: +81-75-724-7517; E-mail: syamada@kit.ac.jp

[b] National Metrology Institute of Japan, National Institute of Advanced Industrial Science and Technology, 1-1-1 Umezono, Tsukuba 305-8560, Japan

[c] Department of Quantum Beam Science, Graduate School of Science and Engineering, Ibaraki University, 4-12-1 Naka-narusawa, Hitachi, Ibaraki 316-8511, Japan

Table of contents

1. NMR Spectra for New Compounds 3a–f

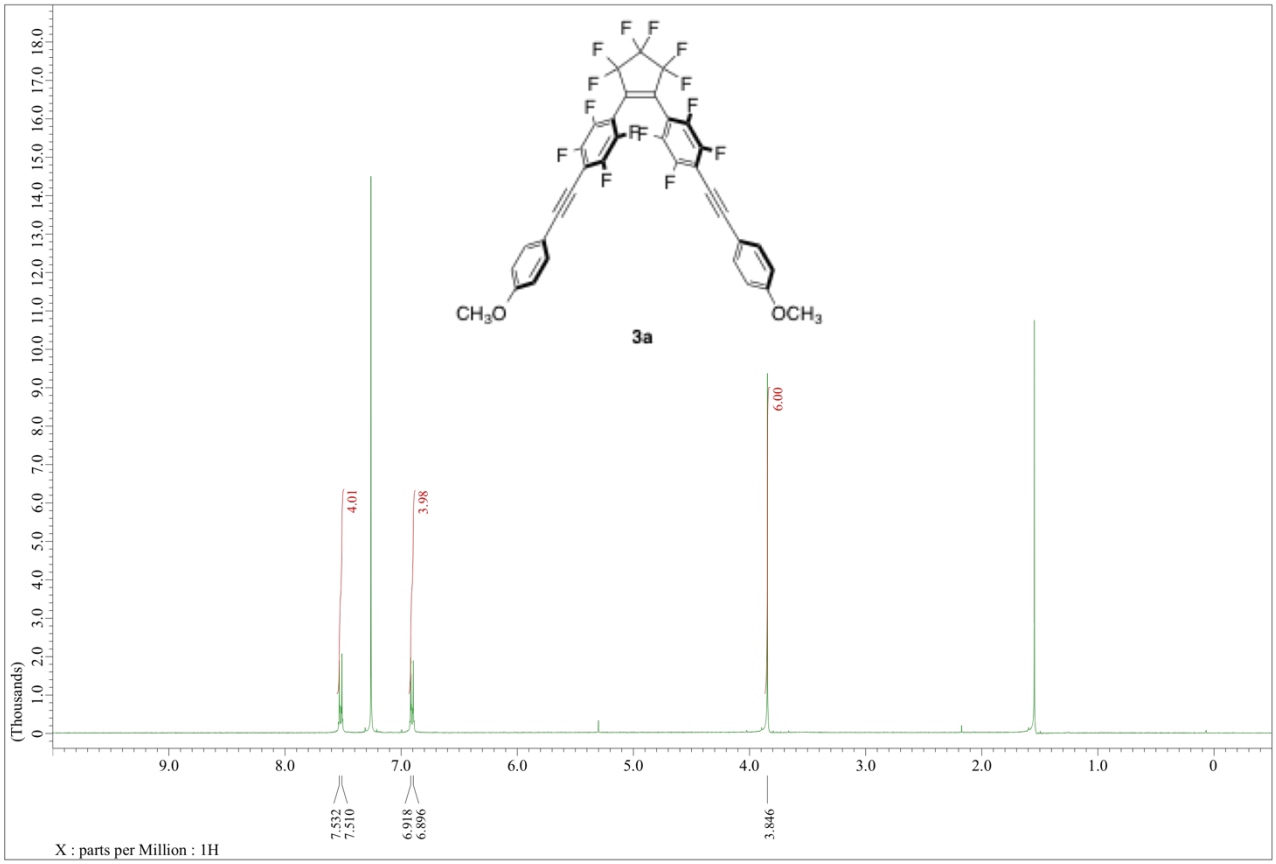

Figure S1. ^{1}H NMR Spectrum of **3a** ($CDCl_3$, 400 MHz)

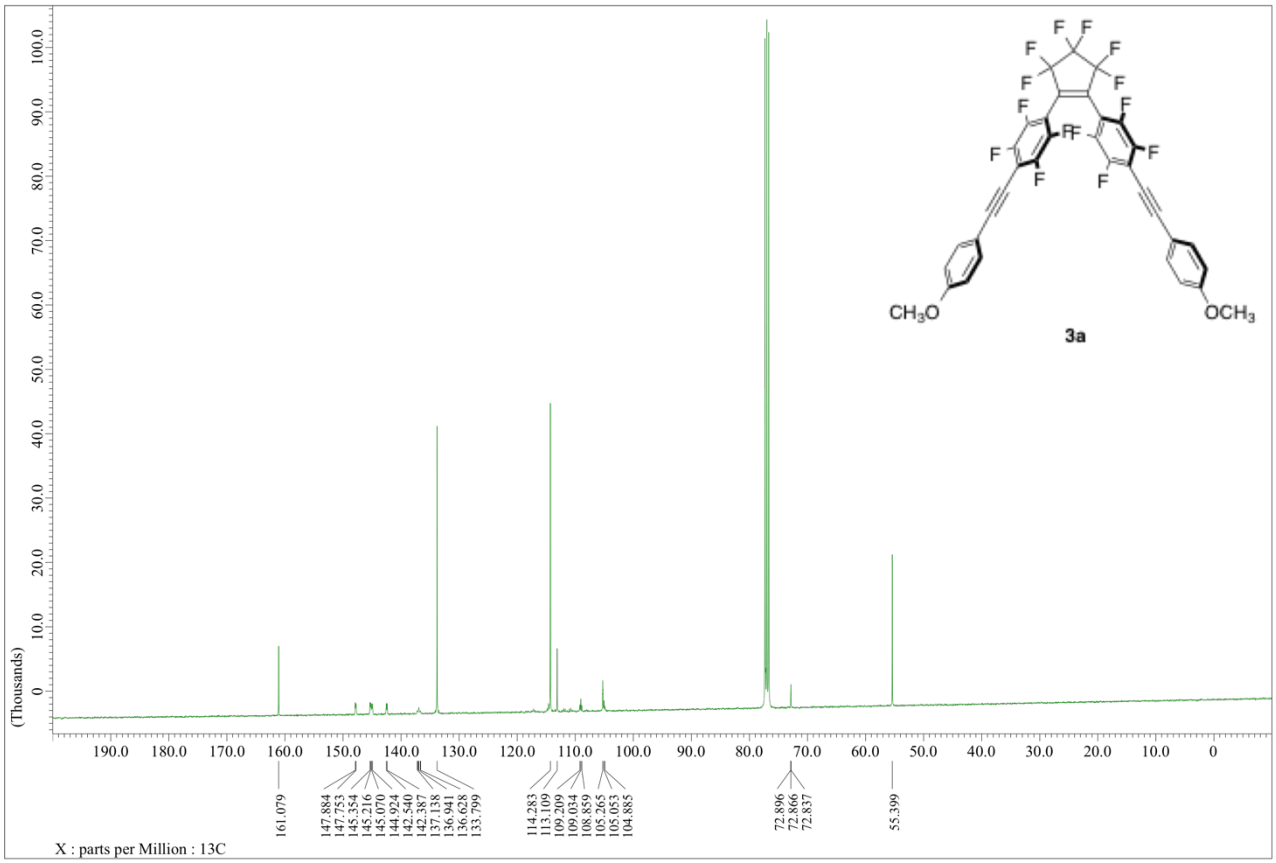

Figure S2. ^{13}C NMR Spectrum of **3a** ($CDCl_3$, 100 MHz)

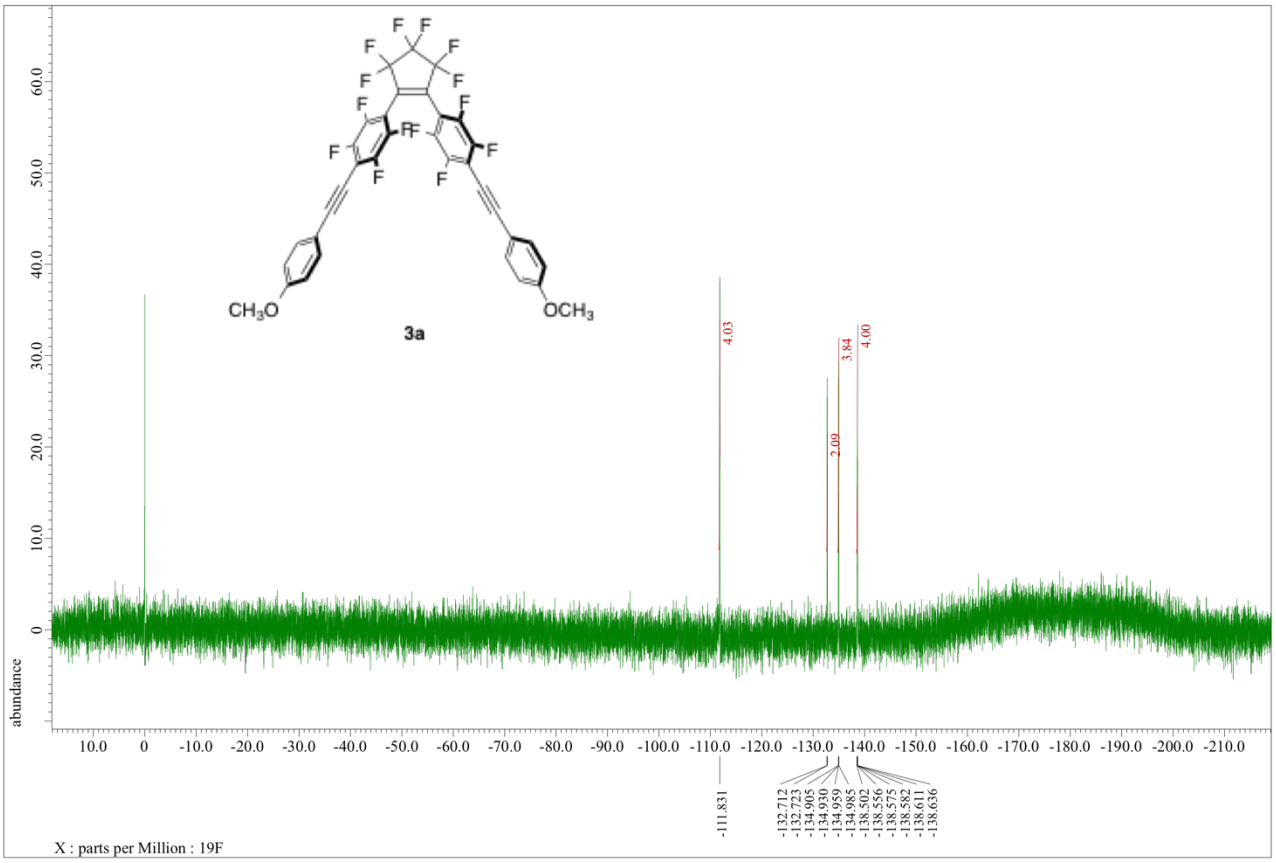

Figure S3. ^{19}F NMR Spectrum of **3a** ($CDCl_3$, 375 MHz)

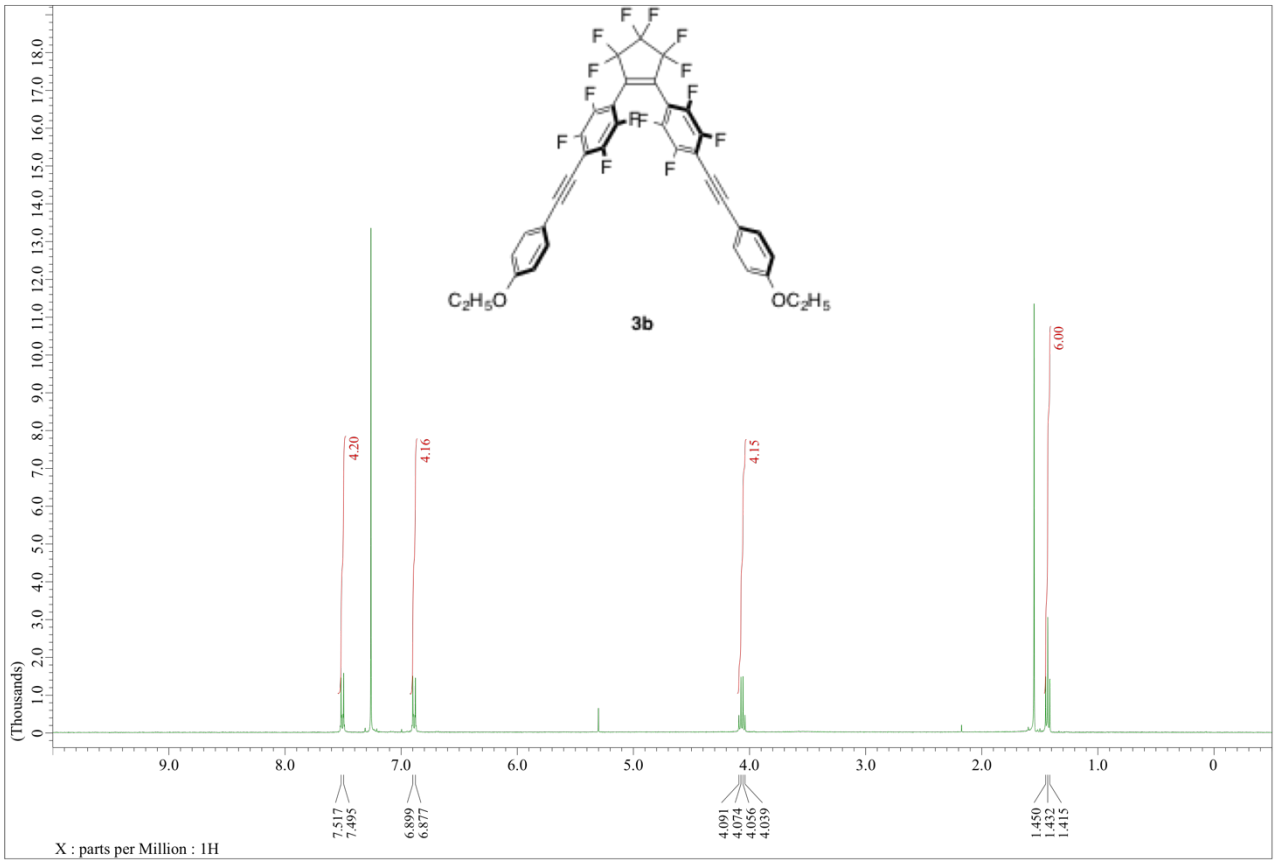

Figure S4. ^{1}H NMR Spectrum of **3b** ($CDCl_3$, 400 MHz)

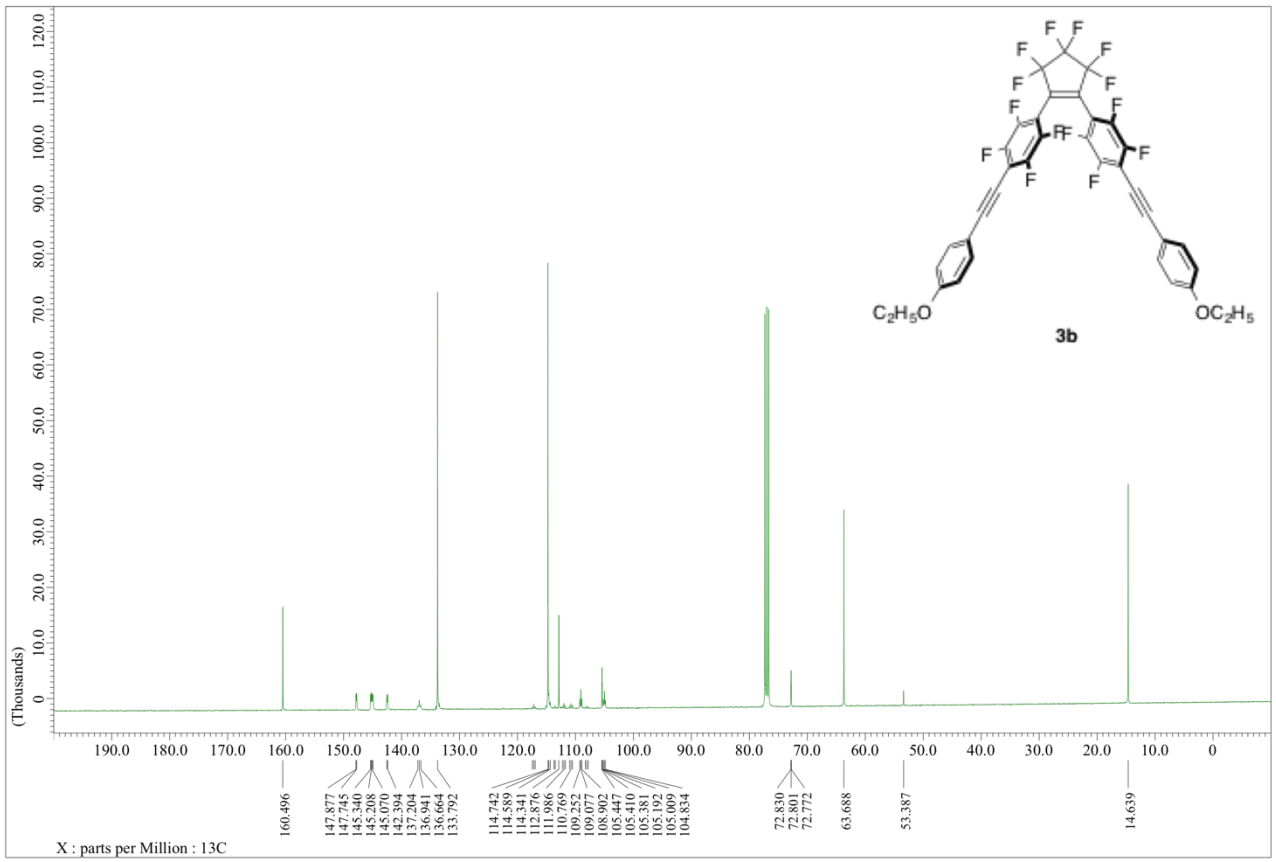

Figure S5. ^{13}C NMR Spectrum of **3b** ($CDCl_3$, 100 MHz)

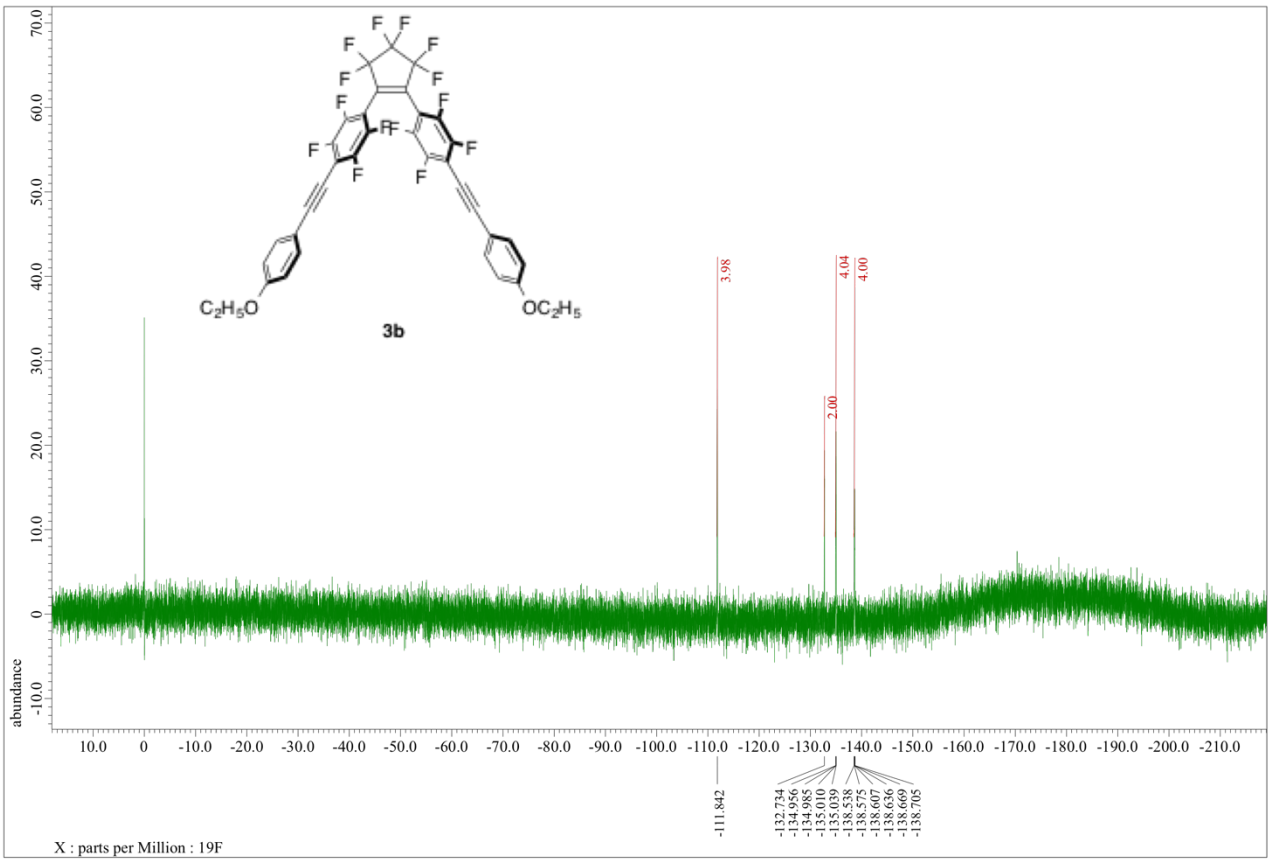

Figure S6. ^{19}F NMR Spectrum of **3b** ($CDCl_3$, 375 MHz)

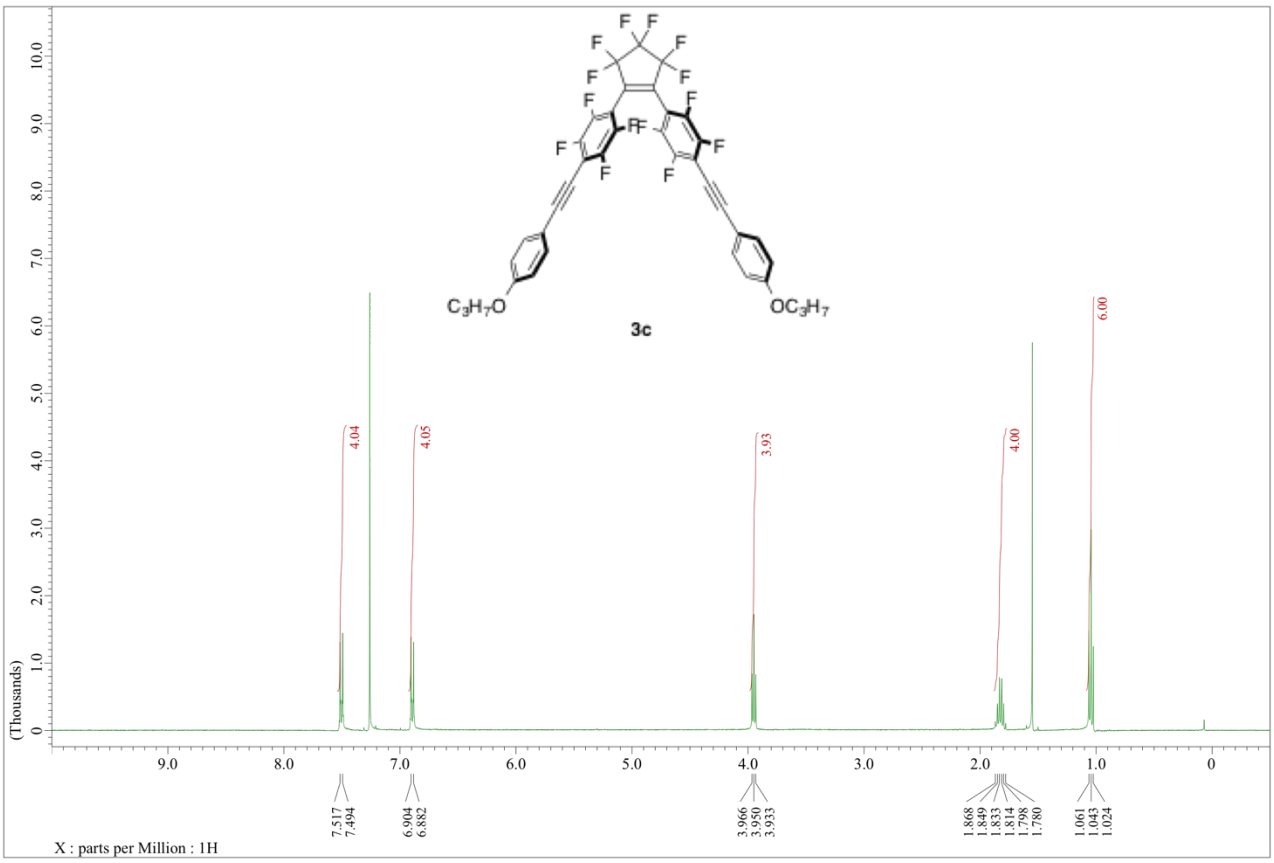

Figure S7. ^{1}H NMR Spectrum of **3c** ($CDCl_3$, 400 MHz)

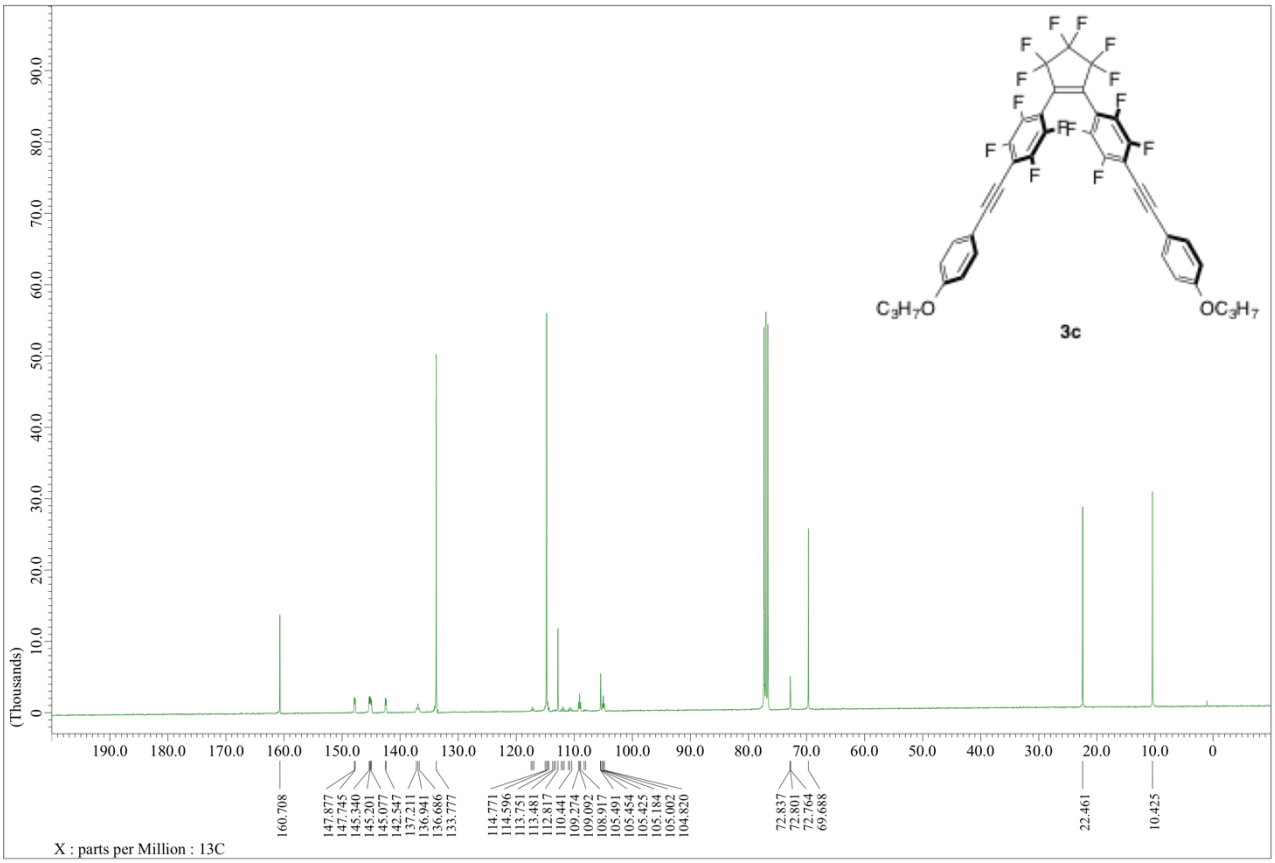

Figure S8. ^{13}C NMR Spectrum of **3c** ($CDCl_3$, 100 MHz)

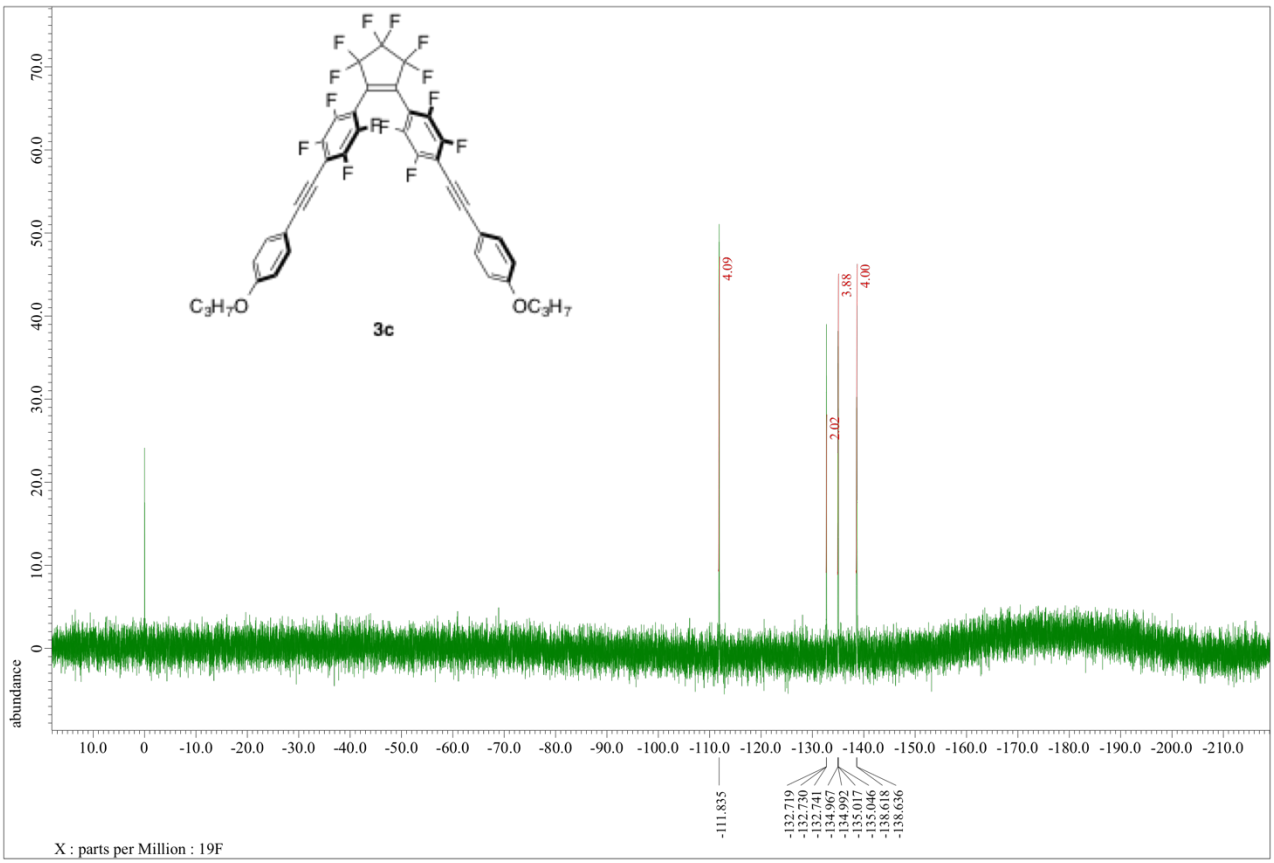

Figure S9. ^{19}F NMR Spectrum of **3c** ($CDCl_3$, 375 MHz)

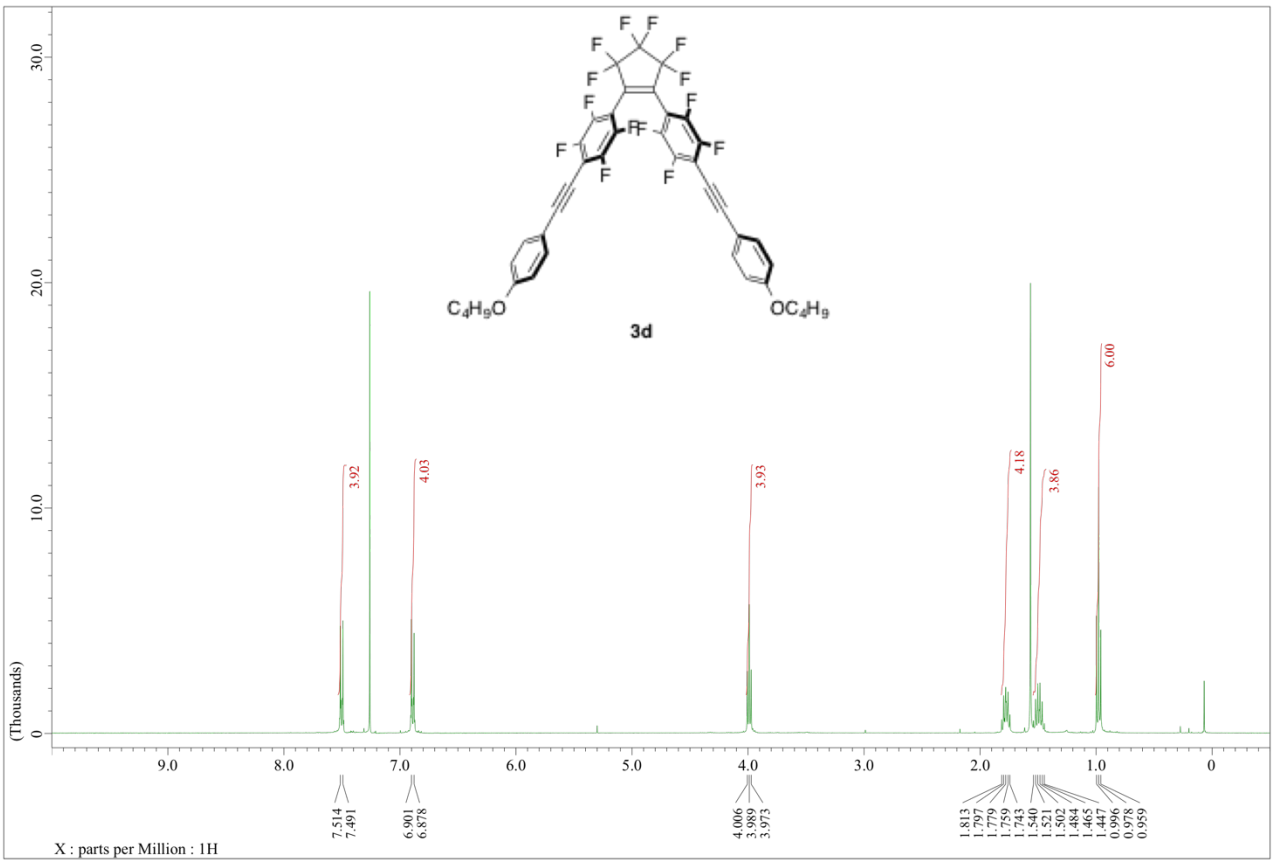

Figure S10. ^{1}H NMR Spectrum of **3d** ($CDCl_3$, 400 MHz)

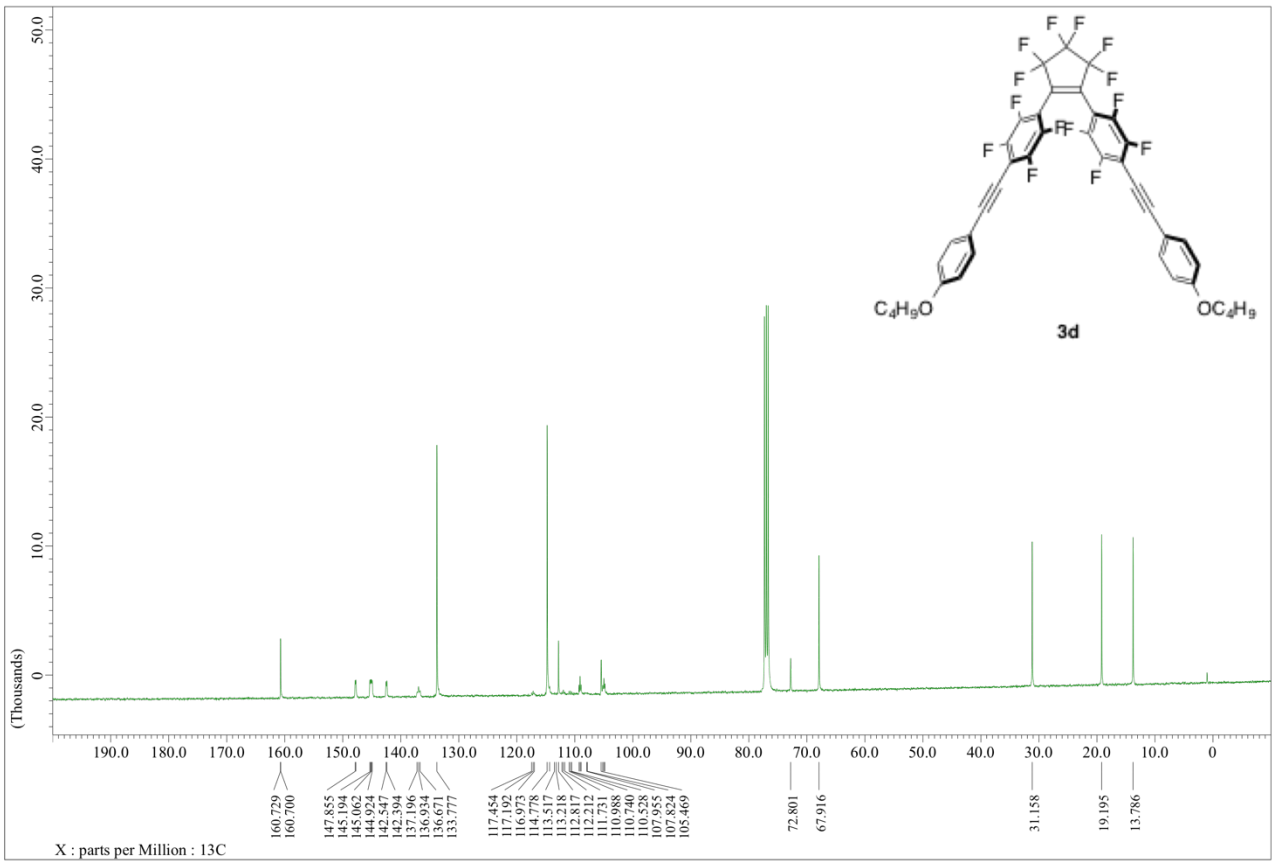

Figure S11. ^{13}C NMR Spectrum of **3d** ($CDCl_3$, 100 MHz)

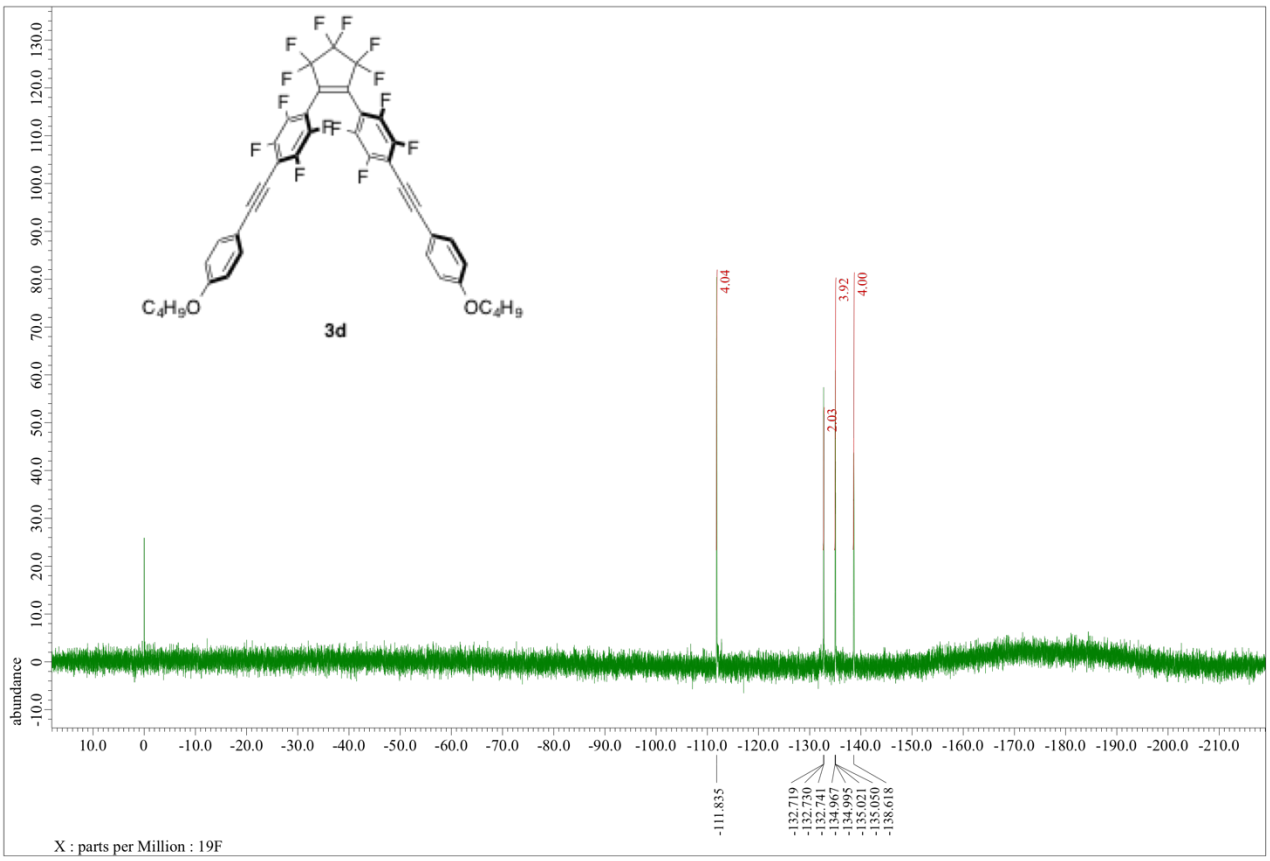

Figure S12. ^{19}F NMR Spectrum of **3d** ($CDCl_3$, 375 MHz)

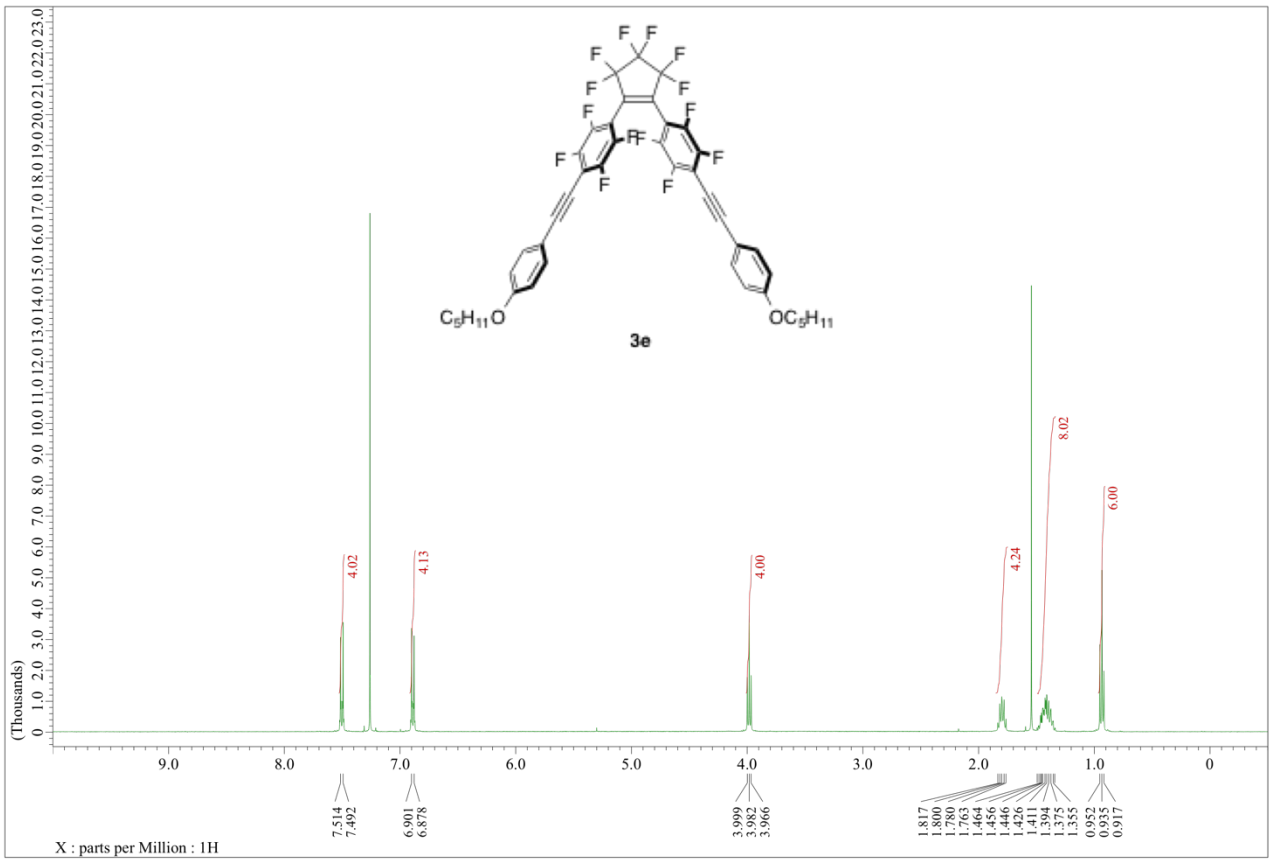

Figure S13. ^{1}H NMR Spectrum of **3e** ($CDCl_3$, 400 MHz)

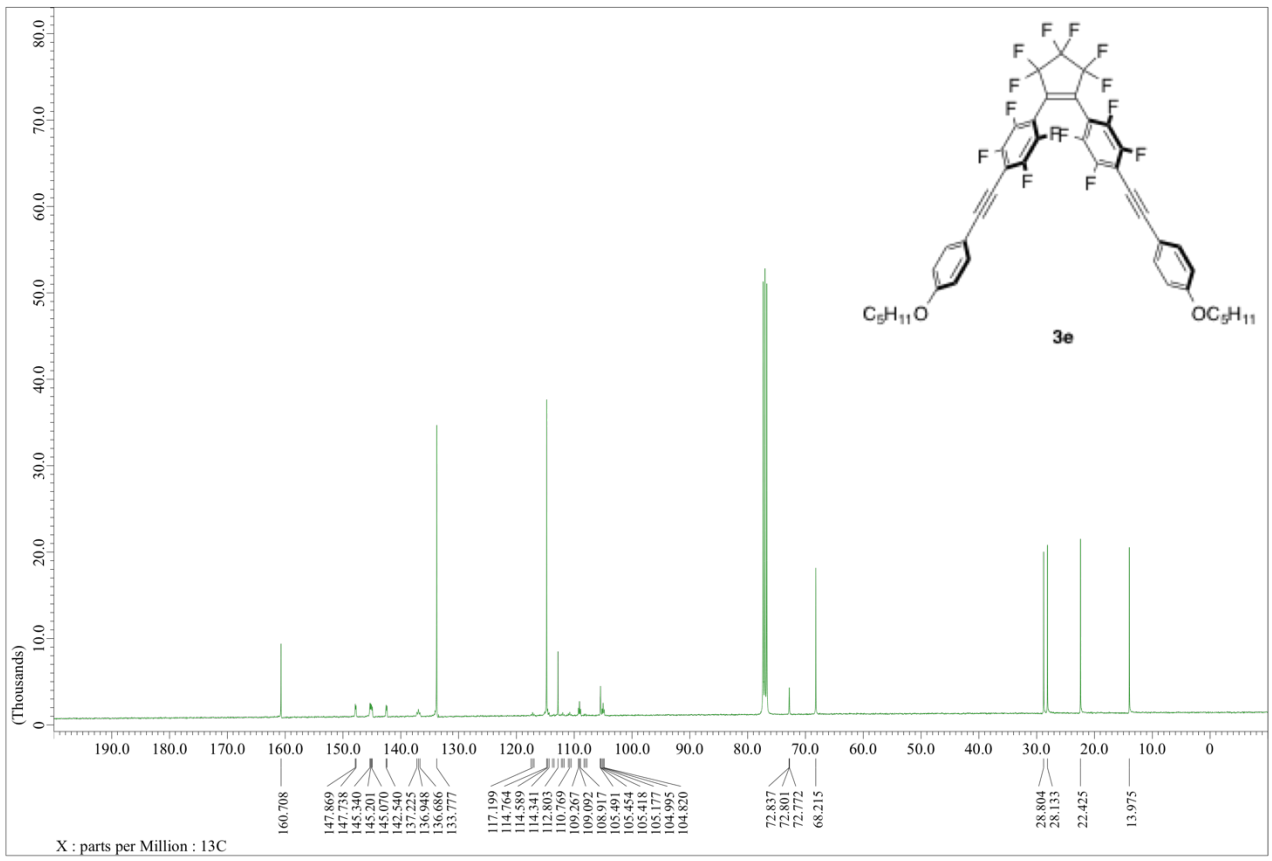

Figure S14. ^{13}C NMR Spectrum of **3e** ($CDCl_3$, 100 MHz)

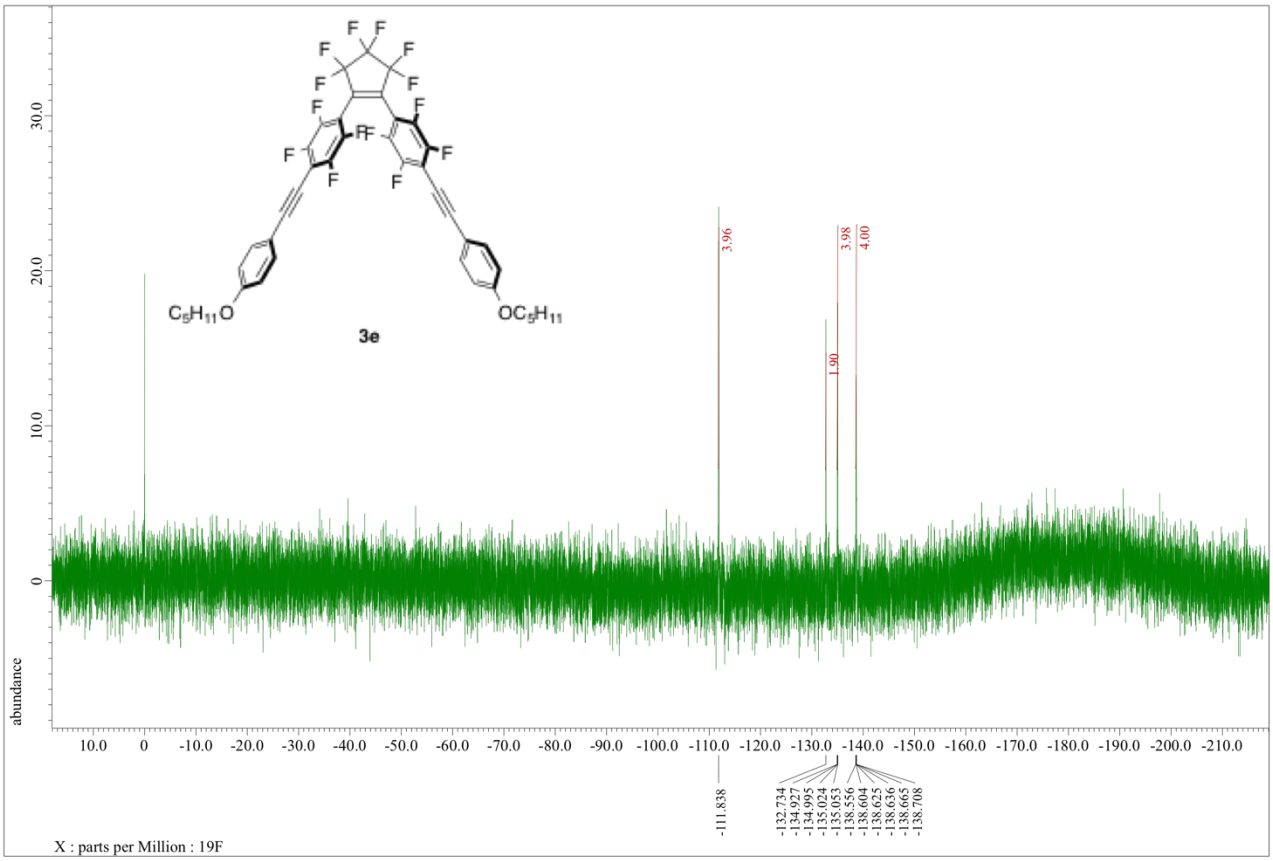

Figure S15. ^{19}F NMR Spectrum of **3e** ($CDCl_3$, 375 MHz)

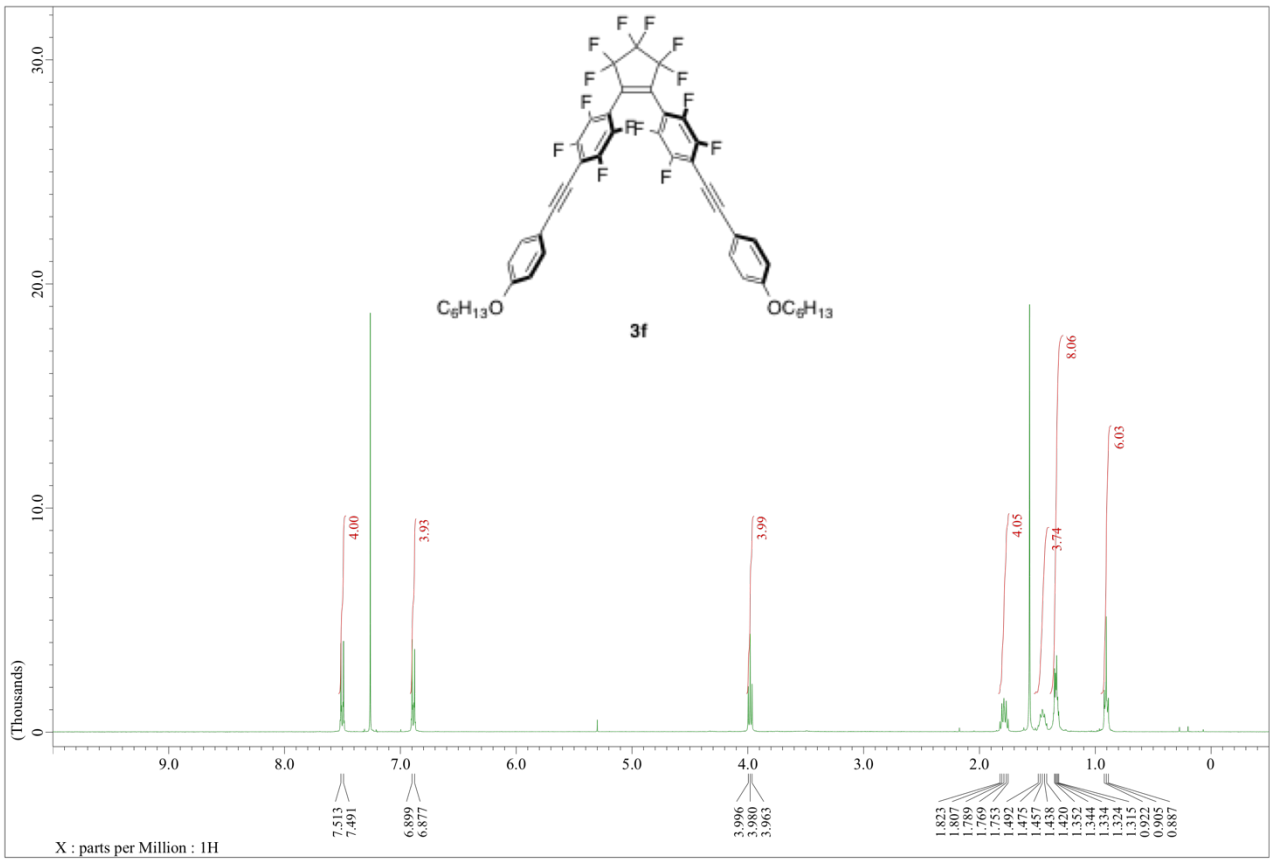

Figure S16. ^{1}H NMR Spectrum of **3f** ($CDCl_3$, 400 MHz)

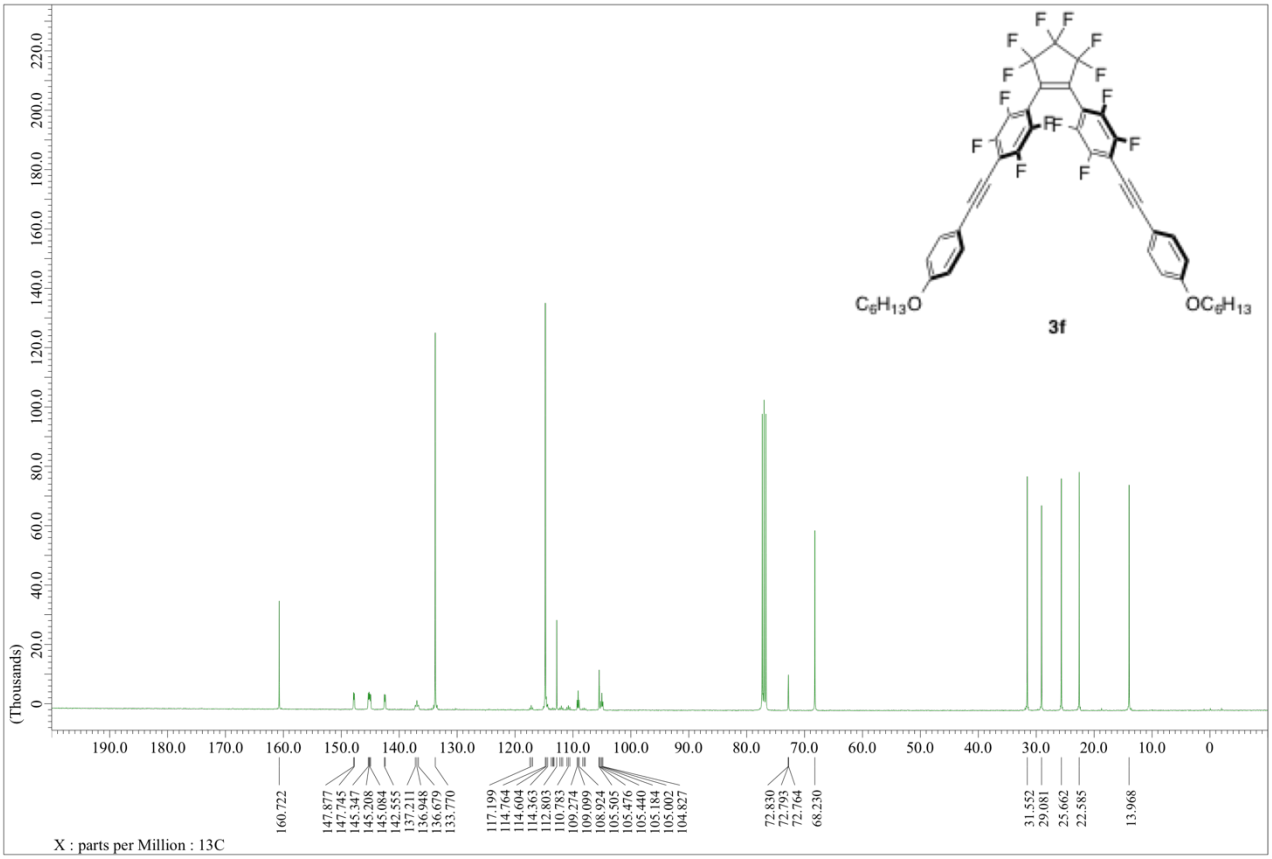

Figure S17. ^{13}C NMR Spectrum of **3f** ($CDCl_3$, 100 MHz)

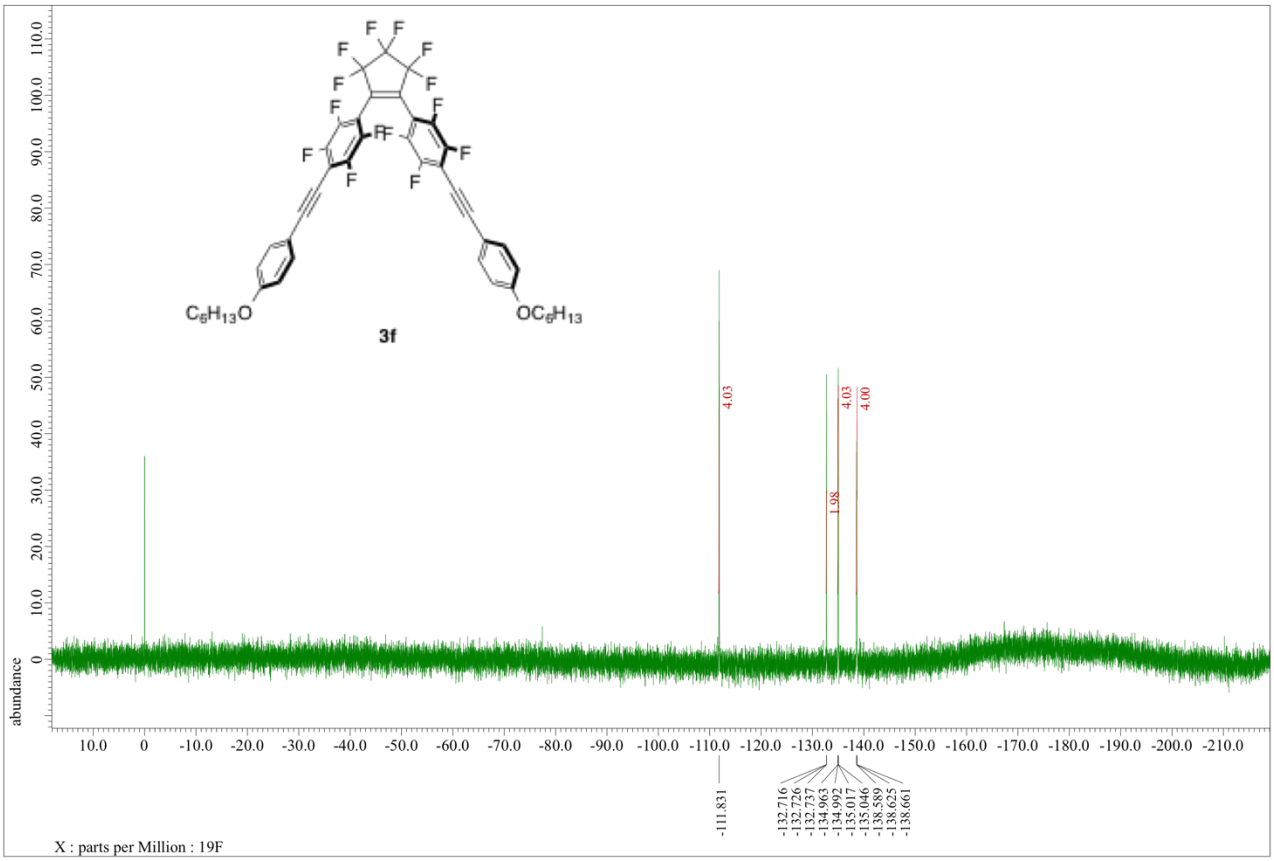

Figure S18. ^{19}F NMR Spectrum of **3f** ($CDCl_3$, 375 MHz)

2. Quantum Chemical Calculation

All computations were carried out using density functional theory (DFT) with the Gaussian 09 (Rev. C.01) package. Geometry optimizations were executed using the CAM-B3LYP hybrid functional and 6-31G(d) basis set. Vertical excitations and optimizations at the excited state were also calculated using a TD-DFT method at the same level of theory.

<Under gas phase>

(a) Optimized structure in S0 state

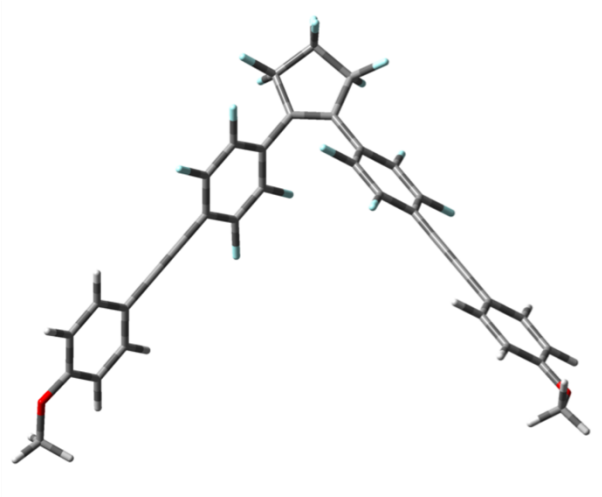

(b) Electrostatic potential diagram in S0 state

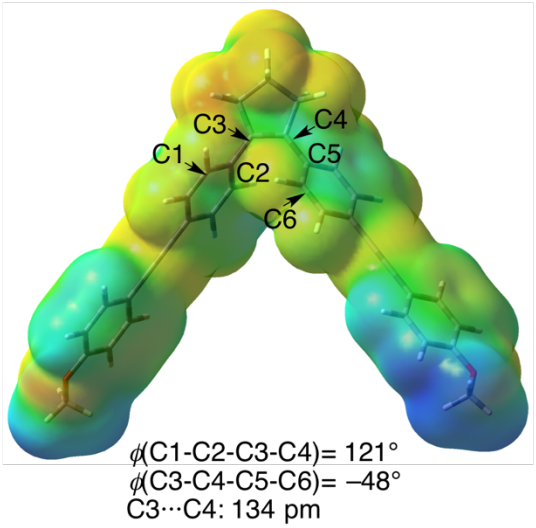

SCF Done: E(RCAM-B3LYP) = –2889.05471951
Dipole moment (Debye): X = –0.1309, Y = 9.1871, Z = 0.0436, Tot = 9.1881

(c) Optimized structure in S1 state

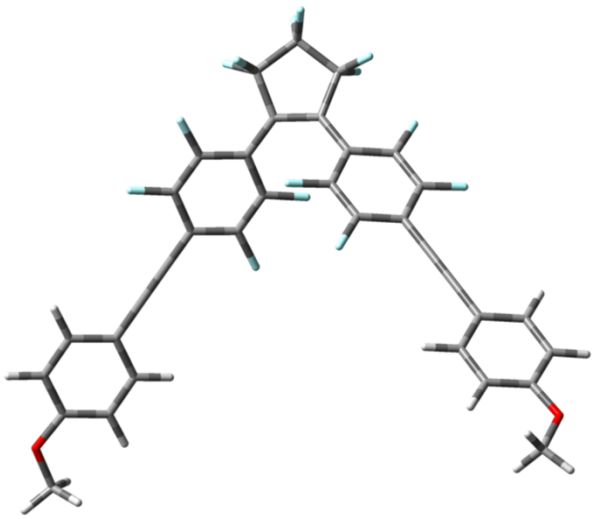

(d) Electrostatic potenstial diagram in S1 state

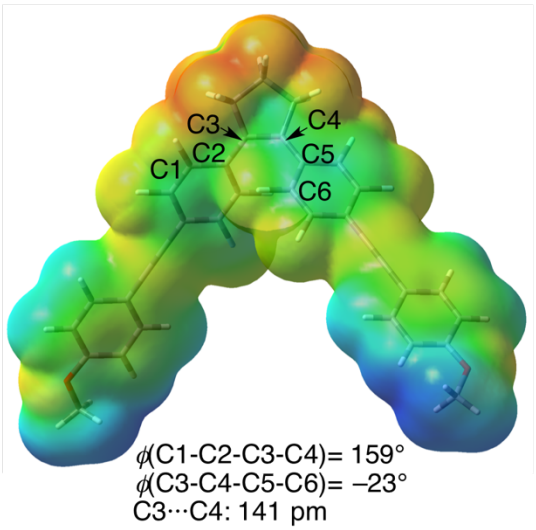

SCF Done: E(RCAM-B3LYP) = –2889.03647378
Dipole moment (Debye): X = 0.0048, Y = 11.3361, Z = –0.0052, Tot = 11.3361

Figure 19. (a) Optimized structure of **3a** in S_0 state and (b) the electrostatic potential diagram. (c) Optimized structure of **3a** in S_1 state and (d) the electrostatic potential diagram.

<Under CPCM (CH_2Cl_2) conditions>

(a) Optimized structure in S_0 state

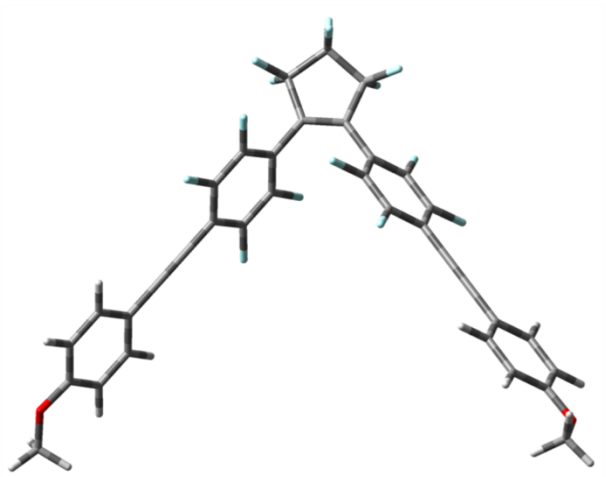

(b) Electrostatic potential diagram in S_0 state

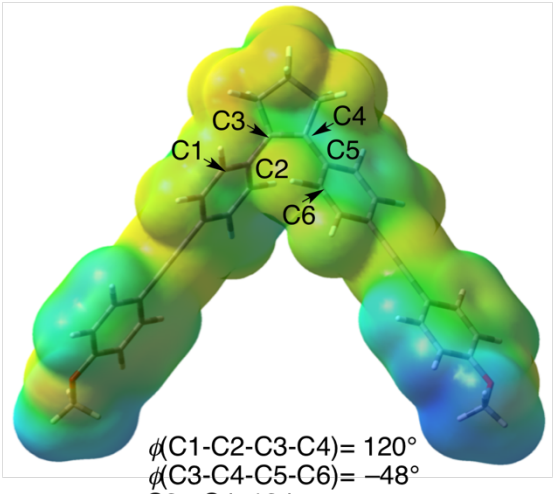

SCF Done: E(RCAM-B3LYP) = –2889.06662217
Dipole moment (Debye): X = –0.1421, Y = 10.5112, Z = 0.0375, Tot = 10.5123

(c) Optimized structure in S_1 state

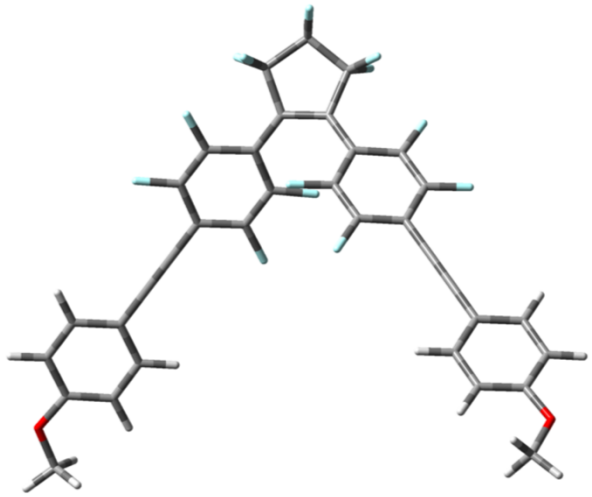

(d) Electrostatic potential diagram in S_1 state

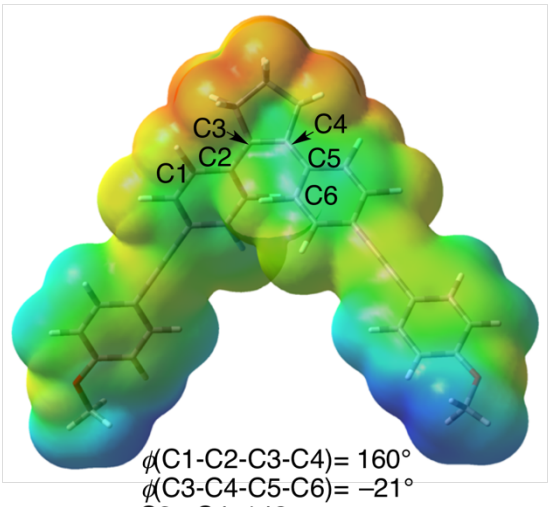

SCF Done: E(RCAM-B3LYP) = –2889.04620574
Dipole moment (Debye): X = –0.0008, Y = 13.5608, Z = 0.0004, Tot = 13.5608

Figure 20. (a) Optimized structure of **3a** calculated by DFT and TD-DFT method with a CPCM (CH_2Cl_2) model in S_0 state and (b) the electrostatic potential diagram. (c) Optimized structure of **3a** in S_1 state and (d) the electrostatic potential diagram.

Frontier molecular orbitals

<S_0 state under gas phase>

(a)HOMO–1 (–7.21 eV)

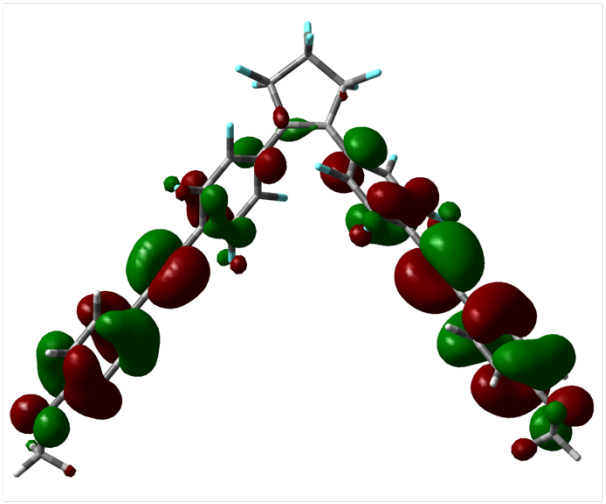

(b) HOMO (–7.13 eV)

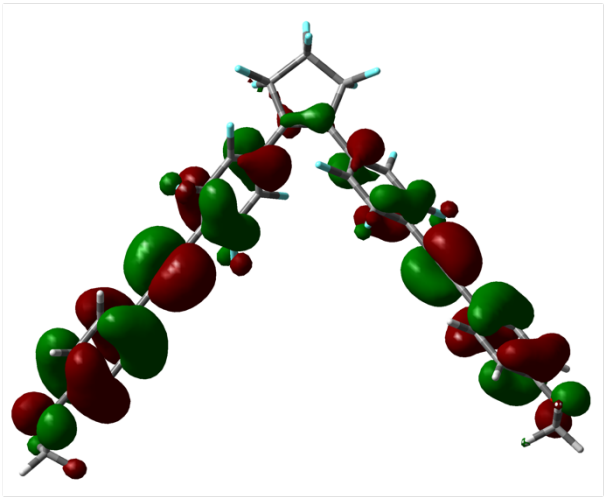

(c) LUMO (–1.30 eV)

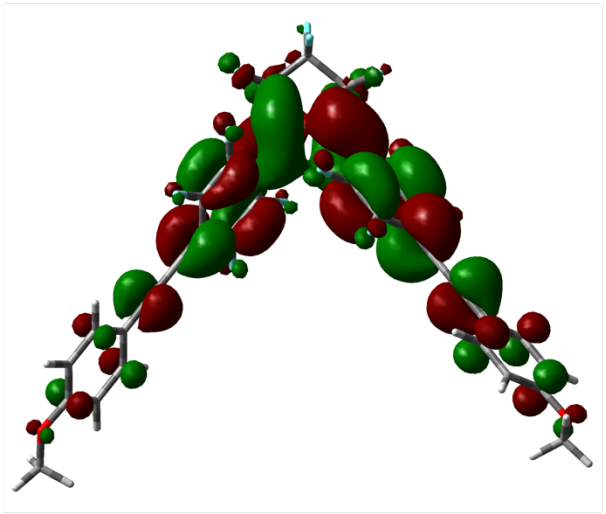

(d) LUMO+1 (–0.61 eV)

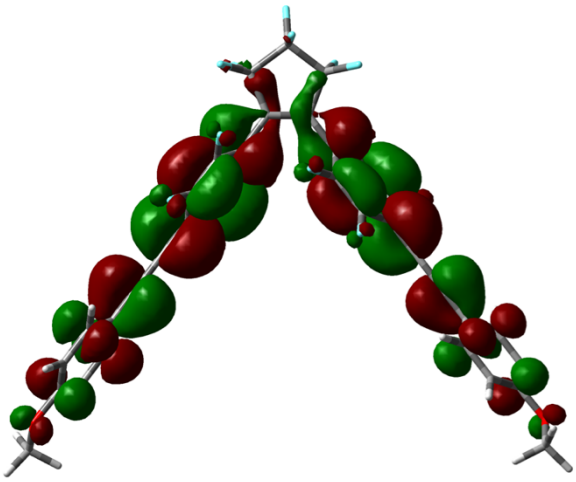

Excitation energies and oscillator strengths:

Excited State 1: Singlet-A 3.7941 eV 326.78 nm f=1.1158 <S**2>=0.000

177 ->184 0.14685

182 ->184 –0.13074

182 ->185 0.31761

183 ->184 0.56017

183 ->186 0.10379

This state for optimization and/or second-order correction.

Total Energy, E(TD-HF/TD-KS) = –2889.07446098

Copying the excited state density for this state as the 1-particle RhoCI density.

Excited State 2: Singlet-A 4.0516 eV 306.01 nm f=1.2985 <S**2>=0.000

176 ->184 0.12456

182 ->184 0.54605

182 ->186 0.12142

183 ->185 0.36658

<S_1 state under gas phase>

(e) HOMO–1 (–7.23 eV)

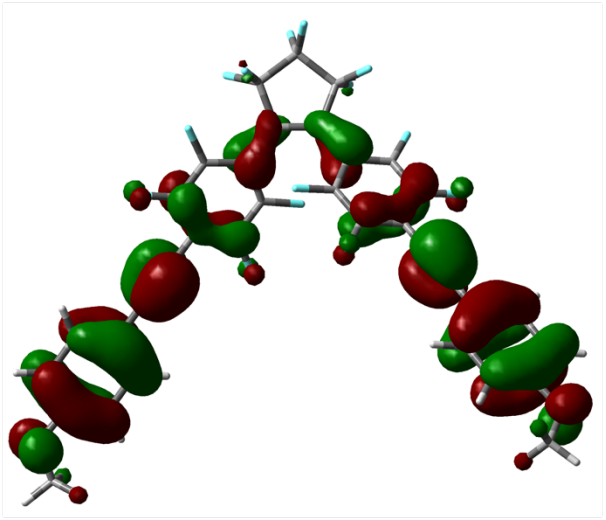

(f) HOMO (–6.85 eV)

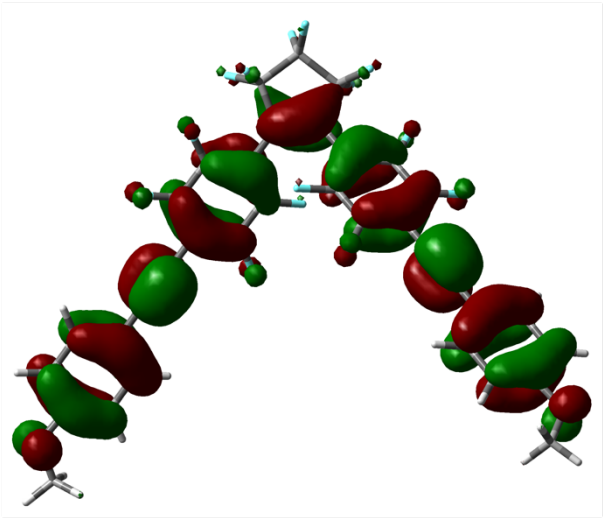

(g) LUMO (–2.16 eV)

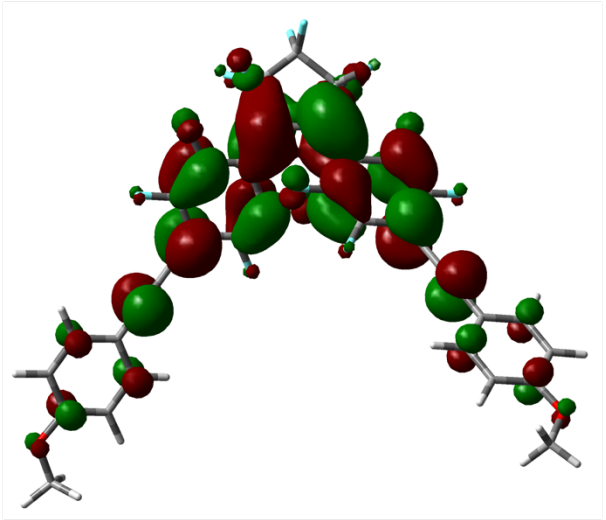

Excitation energies and oscillator strengths:

Excited State 1: Singlet-A 2.8237 eV 439.09 nm f=1.3127 <S**2>=0.000

181 ->184 –0.16969

182 ->185 0.14673

183 ->184 0.66181

This state for optimization and/or second-order correction.

Total Energy, E(TD-HF/TD-KS) = –2888.93270561

Copying the excited state density for this state as the 1-particle RhoCI density.

Excited State 2: Singlet-A 3.5443 eV 349.81 nm f=0.9279 <S**2>=0.000

176 ->184 0.12997

182 ->184 0.66171

183 ->185 0.13363

<S_0 state under CPCM conditions>

(a)HOMO–1 (–7.21 eV)

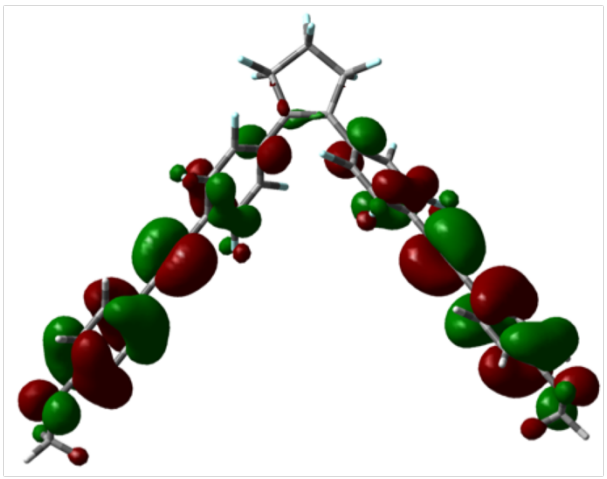

(b) HOMO (–7.13 eV)

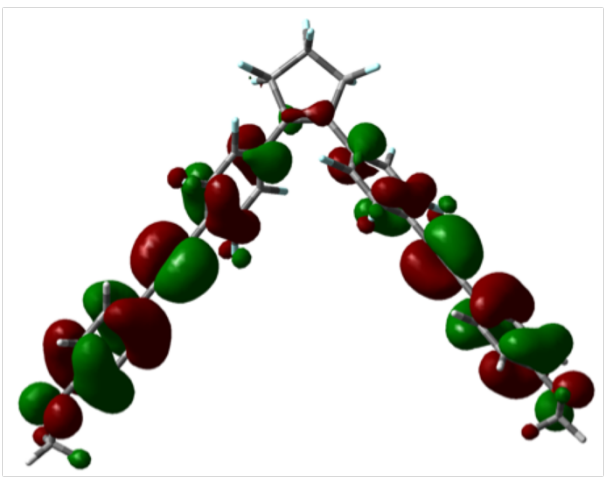

(c) LUMO (–1.37 eV)

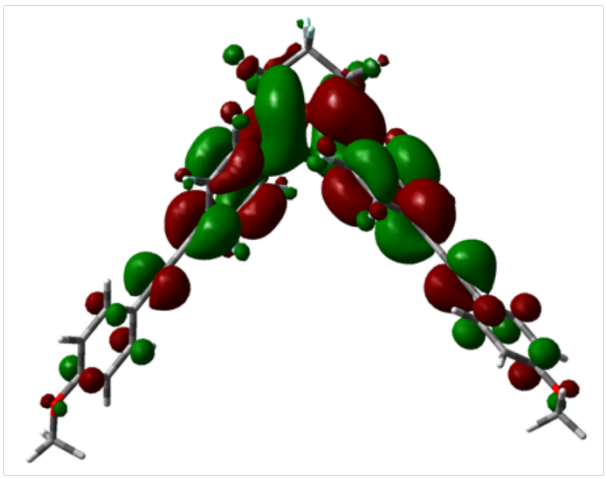

(d) LUMO+1 (–0.66 eV)

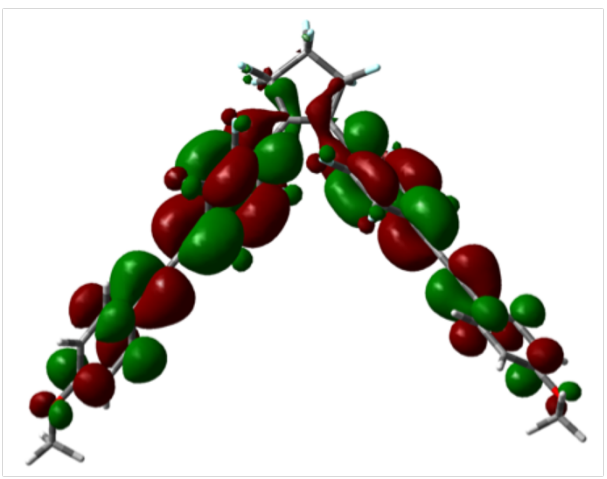

Excitation energies and oscillator strengths:

Excited State	1:	Singlet-A	3.7382 eV	331.67 nm	f=1.2521	<S**2>=0.000
177 ->184		0.10559				
179 ->184		0.15030				
182 ->184		0.14755				
182 ->185		–0.29659				
183 ->184		0.56643				
183 ->186		0.10190				

This state for optimization and/or second-order correction.

Total Energy, E(TD-HF/TD-KS) = –2888.92924492

Copying the excited state density for this state as the 1-particle RhoCI density.

Excited State	2:	Singlet-A	3.9919 eV	310.59 nm	f=1.4840	<S**2>=0.000
176 ->184		0.12953				
182 ->184		0.53794				
182 ->186		0.12795				
183 ->185		–0.37025				

<S_1 state under CPCM conditions >

(e) HOMO–1 (–7.20 eV)

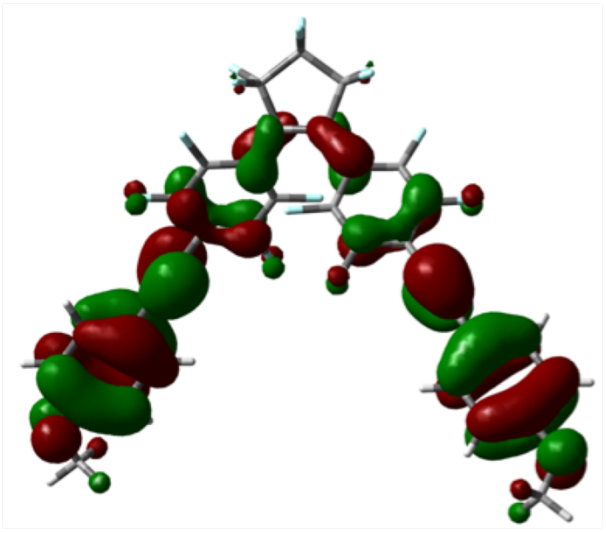

(f) HOMO (–6.82 eV)

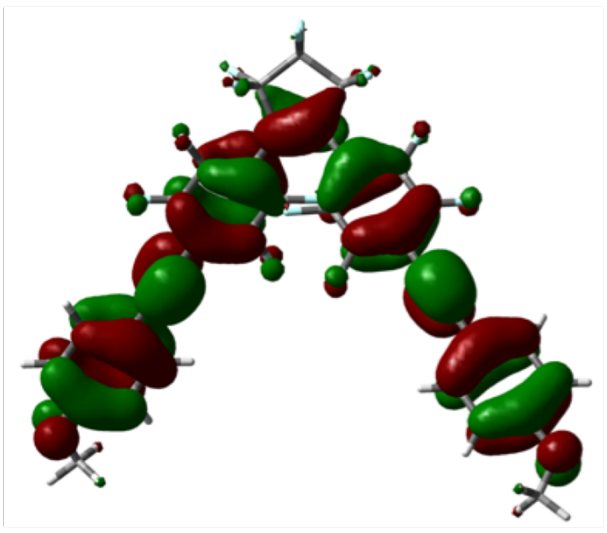

(g) LUMO (–2.31 eV)

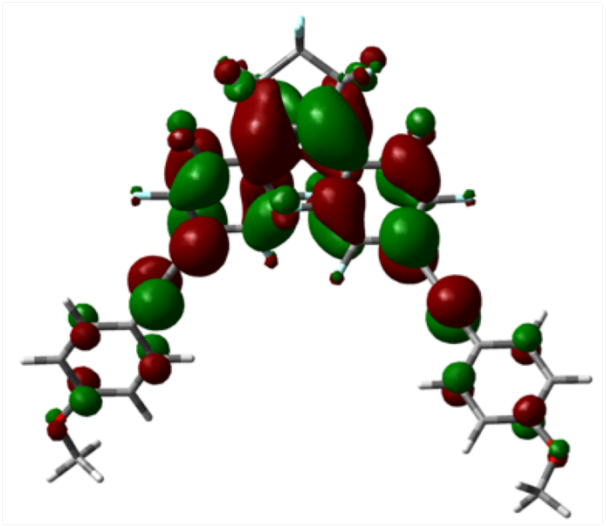

Excitation energies and oscillator strengths:

Excited State	1:	Singlet-A	2.5187 eV	492.25 nm	f=1.5980	<S**2>=0.000
181 ->184		–0.18945				
182 ->185		–0.14172				
183 ->184		0.65856				

This state for optimization and/or second-order correction.

Total Energy, E(TD-HF/TD-DFT) = -2888.95364459

Copying the excited state density for this state as the 1-particle RhoCI density.

Excited State	2:	Singlet-A	3.2249 eV	384.46 nm	f=1.3527	<S**2>=0.000
176 ->184		–0.13969				
182 ->184		0.64468				
183 ->185		–0.20509				

Figure S21. Frontier molecular orbital (HOMO–1, HOMO, LUMO, and/or LUMO+1) in the S_0 and S_1 states and the calculated electronic transition energies (nm) and oscillator strengths.

Table S1. Cartesian coordinate for **3a** at the ground (S_0) state in gas phase

No.	Atom No.	Type	Coordinates (Angstroms) x	y	z
1	9	0	2.728968	-2.980516	2.071780
2	9	0	0.610046	-1.466845	-1.867888
3	9	0	4.324548	-0.854511	2.026456
4	8	0	8.271776	6.504354	-0.060099
5	9	0	2.193933	0.661767	-1.899205
6	9	0	-0.830733	-1.716876	2.103971
7	6	0	4.885729	2.077693	0.009718
8	9	0	-2.232844	-2.776192	-2.271434
9	6	0	2.333588	-0.221445	-0.912723
10	9	0	-2.521153	0.346482	2.147288
11	6	0	6.730926	3.405152	0.949342
12	1	0	6.843536	2.670456	1.739236
13	6	0	7.414049	5.458602	-0.108934
14	6	0	-3.292968	-0.130520	-0.032958
15	6	0	3.414125	-0.991158	1.065483
16	6	0	-0.600761	-3.491397	-0.053024
17	6	0	-1.599225	-1.492532	1.035658
18	6	0	3.311568	-0.021821	0.064659
19	6	0	-5.845705	3.013011	0.036673
20	6	0	5.738743	3.218081	-0.027654
21	6	0	7.556238	4.509014	0.909136
22	1	0	8.326236	4.665704	1.656201
23	6	0	-1.509918	-2.334687	-0.070474
24	6	0	4.161884	1.111055	0.038399
25	6	0	0.728739	-3.475426	0.112243
26	6	0	1.603051	-2.294243	0.115678
27	9	0	-3.934555	-0.725849	-2.224467
28	8	0	-8.488590	6.212232	0.022947
29	6	0	1.505963	-1.328174	-0.886872
30	6	0	8.180556	7.496259	-1.062299
31	1	0	8.363442	7.077311	-2.058664
32	1	0	8.954424	8.228384	-0.831949
33	1	0	7.201267	7.988814	-1.050811
34	6	0	-7.507736	4.391511	-1.051931
35	1	0	-8.126164	4.640260	-1.907059
36	6	0	-8.638882	7.050095	1.150570
37	1	0	-8.992106	6.488411	2.023212
38	1	0	-9.386143	7.794135	0.874900
39	1	0	-7.699559	7.556325	1.401962
40	9	0	-2.053468	-5.110084	-1.039269
41	9	0	-1.688204	-5.234579	1.105363
42	6	0	-1.127793	-4.904591	-0.083387
43	6	0	2.583640	-2.096413	1.086287
44	6	0	5.605811	4.172822	-1.038932
45	1	0	4.843086	4.038090	-1.798335
46	6	0	-2.317640	-2.039974	-1.165732
47	6	0	-4.186911	0.969192	-0.012655
48	6	0	-6.826933	4.893104	1.213214
49	1	0	-6.889045	5.494199	2.111537
50	6	0	-5.954703	3.813556	1.176356
51	1	0	-5.346681	3.584745	2.045001
52	6	0	-4.947882	1.906928	0.009329
53	6	0	-3.189789	-0.966992	-1.147813
54	6	0	-2.471109	-0.419699	1.059175
55	6	0	6.432886	5.286767	-1.085847
56	1	0	6.304818	6.008758	-1.882372
57	6	0	-7.608440	5.186274	0.095352
58	6	0	-6.639493	3.320655	-1.080954
59	1	0	-6.563544	2.705962	-1.971328
60	6	0	0.130349	-5.759224	-0.318710
61	6	0	1.271641	-4.881091	0.231762
62	9	0	0.304792	-5.935213	-1.642262
63	9	0	2.415017	-5.049898	-0.460784
64	9	0	0.063751	-6.952713	0.282913
65	9	0	1.504277	-5.233478	1.516081

Table S2. Cartesian coordinate for **3a** at the excited (S_1) state in gas phase

No.	Atom No.	Type	Coordinates (Angstroms) x	y	z
1	9	0	3.019804	-3.187648	1.830263
2	9	0	0.437018	-1.142857	-1.608924
3	9	0	4.726521	-1.186638	1.706359
4	8	0	8.736576	6.172185	-0.191667
5	9	0	2.130829	0.867032	-1.658660
6	9	0	-0.434650	-1.139510	1.604753
7	6	0	5.157869	1.927210	-0.053543
8	9	0	-3.028007	-3.192498	-1.822086
9	6	0	2.338543	-0.121741	-0.788905
10	9	0	-2.126976	0.870857	1.653425
11	6	0	7.193606	3.052953	0.725577
12	1	0	7.377264	2.231870	1.409722
13	6	0	7.825516	5.179133	-0.214971
14	6	0	-3.485685	-0.077651	-0.030635
15	6	0	3.668556	-1.178333	0.896515
16	6	0	-0.676729	-3.340604	-0.198299
17	6	0	-1.451043	-1.160486	0.736114
18	6	0	3.484775	-0.078131	0.031138
19	6	0	-6.051557	3.014861	0.105247
20	6	0	6.052101	3.013143	-0.105196
21	6	0	8.062984	4.116765	0.670456
22	1	0	8.943335	4.161360	1.301698
23	6	0	-1.606802	-2.268271	-0.146636
24	6	0	4.380933	0.989965	-0.011969
25	6	0	0.675701	-3.340318	0.198091
26	6	0	1.605582	-2.267936	0.146823
27	9	0	-4.732893	-1.190705	-1.698737
28	8	0	-8.734719	6.175033	0.191501
29	6	0	1.451834	-1.162053	-0.738458
30	6	0	8.562893	7.276538	-1.059687
31	1	0	8.575427	6.963427	-2.109648
32	1	0	9.405489	7.940913	-0.870293
33	1	0	7.627307	7.806202	-0.847806
34	6	0	-8.064879	4.116696	-0.666582
35	1	0	-8.947504	4.159584	-1.294760
36	6	0	-8.557614	7.281997	1.055486
37	1	0	-8.566471	6.972118	2.106443
38	1	0	-9.400697	7.946034	0.867071
39	1	0	-7.622646	7.810738	0.838627
40	9	0	-1.102760	-4.902354	-1.946522
41	9	0	-2.305231	-5.084333	-0.131986
42	6	0	-1.084550	-4.732726	-0.598401
43	6	0	2.782320	-2.219766	0.947270
44	6	0	5.827591	4.084674	-0.986694
45	1	0	4.954038	4.063530	-1.629127
46	6	0	-2.786401	-2.221955	-0.943174
47	6	0	-4.381381	0.990848	0.012289
48	6	0	-6.695329	5.162005	1.041216
49	1	0	-6.493144	5.974449	1.727654
50	6	0	-5.823533	4.089070	0.982569
51	1	0	-4.947672	4.069651	1.621908
52	6	0	-5.157871	1.928459	0.053780
53	6	0	-3.672215	-1.180130	-0.892463
54	6	0	-2.337267	-0.119739	0.786362
55	6	0	6.699947	5.157136	-1.045561
56	1	0	6.500510	5.967490	-1.735264
57	6	0	-7.823877	5.181757	0.214635
58	6	0	-7.196033	3.052439	-0.721518
59	1	0	-7.382431	2.229270	-1.402403
60	6	0	0.002277	-5.666298	-0.003362
61	6	0	1.083305	-4.731791	0.600090
62	9	0	0.542300	-6.443723	-0.957293
63	9	0	2.307788	-5.081440	0.142508
64	9	0	-0.532069	-6.457704	0.942088
65	9	0	1.091763	-4.901894	1.948354

Table S3. Cartesian coordinate for **3a** at the excited (S_0) state with a CPCM (CH_2Cl_2) model

No.	Atom No.	Type	Coordinates (Angstroms) x	y	z
1	9	0	2.732271	-2.977051	2.069251
2	9	0	0.611674	-1.470309	-1.873420
3	9	0	4.325581	-0.850276	2.020998
4	8	0	8.286131	6.495490	-0.045351
5	9	0	2.195740	0.657749	-1.909068
6	9	0	-0.843444	-1.725479	2.115740
7	6	0	4.888042	2.078733	0.002231
8	9	0	-2.219179	-2.757448	-2.275654
9	6	0	2.335079	-0.223885	-0.919799
10	9	0	-2.528984	0.340657	2.159377
11	6	0	6.722402	3.406331	0.961345
12	1	0	6.823313	2.677487	1.758203
13	6	0	7.427214	5.453087	-0.099744
14	6	0	-3.287401	-0.121886	-0.028536
15	6	0	3.414566	-0.988629	1.058722
16	6	0	-0.600718	-3.487456	-0.051435
17	6	0	-1.602437	-1.492734	1.042346
18	6	0	3.312343	-0.021101	0.056803
19	6	0	-5.851315	3.014673	0.038114
20	6	0	5.744289	3.217347	-0.030121
21	6	0	7.551384	4.508199	0.926524
22	1	0	8.309586	4.663685	1.686023
23	6	0	-1.507128	-2.328510	-0.067415
24	6	0	4.162804	1.112146	0.029498
25	6	0	0.729424	-3.474230	0.110855
26	6	0	1.604651	-2.293924	0.111656
27	9	0	-3.916680	-0.704779	-2.227940
28	8	0	-8.515150	6.194912	0.019059
29	6	0	1.507471	-1.329944	-0.892456
30	6	0	8.212588	7.485847	-1.059283
31	1	0	8.408419	7.057323	-2.047722
32	1	0	8.985589	8.215733	-0.821422
33	1	0	7.235040	7.979143	-1.062372
34	6	0	-7.538123	4.366112	-1.046106
35	1	0	-8.169190	4.595237	-1.897678
36	6	0	-8.655472	7.051095	1.142089
37	1	0	-8.990222	6.496357	2.024825
38	1	0	-9.412609	7.784444	0.866746
39	1	0	-7.716000	7.565827	1.368942
40	9	0	-2.046242	-5.100703	-1.056622
41	9	0	-1.711250	-5.229377	1.092509
42	6	0	-1.132042	-4.897570	-0.087370
43	6	0	2.585191	-2.093302	1.081081
44	6	0	5.628581	4.167439	-1.049706
45	1	0	4.877578	4.033222	-1.820741
46	6	0	-2.308153	-2.025916	-1.164752
47	6	0	-4.182442	0.977460	-0.007631
48	6	0	-6.827262	4.905944	1.203057
49	1	0	-6.879510	5.519627	2.093151
50	6	0	-5.948767	3.831671	1.168783
51	1	0	-5.327804	3.621980	2.033063
52	6	0	-4.947582	1.912820	0.013420
53	6	0	-3.177951	-0.952529	-1.146535
54	6	0	-2.472554	-0.419083	1.065764
55	6	0	6.459414	5.278597	-1.091008
56	1	0	6.345417	5.996209	-1.893252
57	6	0	-7.627870	5.177460	0.091840
58	6	0	-6.662981	3.300224	-1.073144
59	1	0	-6.598062	2.674919	-1.956983
60	6	0	0.123613	-5.760534	-0.307222
61	6	0	1.270248	-4.879790	0.228231
62	9	0	0.298094	-5.966893	-1.626329
63	9	0	2.406983	-5.056269	-0.473332
64	9	0	0.050409	-6.943044	0.318526
65	9	0	1.516801	-5.231156	1.512515

Table S4. Cartesian coordinate for **3a** at the excited (S_1) state with a CPCM (CH_2Cl_2) model

No.	Atom No.	Type	Coordinates (Angstroms) x	y	z
1	9	0	-2.999261	-3.138530	-1.882477
2	9	0	-0.467323	-1.032912	1.562630
3	9	0	-4.758503	-1.190962	-1.748906
4	8	0	-9.010211	6.003200	0.208411
5	9	0	-2.214854	0.925455	1.620654
6	9	0	0.467262	-1.032853	-1.562531
7	6	0	-5.288200	1.895364	0.036585
8	9	0	2.999435	-3.138638	1.882311
9	6	0	-2.398731	-0.067663	0.749446
10	9	0	2.214808	0.925452	-1.620628
11	6	0	-7.368228	2.943419	-0.726134
12	1	0	-7.529629	2.117682	-1.410124
13	6	0	-8.067257	5.046094	0.222913
14	6	0	3.552474	-0.052104	0.065181
15	6	0	-3.702342	-1.155399	-0.934808
16	6	0	0.675366	-3.257223	0.216889
17	6	0	1.486233	-1.082045	-0.697025
18	6	0	-3.552416	-0.052041	-0.065279
19	6	0	6.218792	2.946564	-0.096789
20	6	0	-6.218751	2.946587	0.096707
21	6	0	-8.274179	3.974930	-0.662612
22	1	0	-9.159870	3.985479	-1.287799
23	6	0	1.612744	-2.198925	0.181556
24	6	0	-4.478547	0.984169	-0.013579
25	6	0	-0.675368	-3.257201	-0.216853
26	6	0	-1.612736	-2.198911	-0.181531
27	9	0	4.758685	-1.191106	1.748659
28	8	0	9.010153	6.003281	-0.208301
29	6	0	-1.486256	-1.082045	0.697070
30	6	0	-8.868855	7.120568	1.077053
31	1	0	-8.861775	6.805569	2.125016
32	1	0	-9.736703	7.751789	0.892079
33	1	0	-7.955019	7.679410	0.853151
34	6	0	8.274182	3.974931	0.662597
35	1	0	9.159868	3.985471	1.287792
36	6	0	8.868688	7.120751	-1.076787
37	1	0	8.861648	6.805900	-2.124796
38	1	0	9.736467	7.752040	-0.891722
39	1	0	7.954792	7.679470	-0.852820
40	9	0	1.034536	-4.824141	1.984798
41	9	0	2.299170	-5.013009	0.215121
42	6	0	1.062947	-4.646877	0.633782
43	6	0	-2.790217	-2.170324	-0.987101
44	6	0	-6.024757	4.026028	0.979219
45	1	0	-5.146608	4.038431	1.615315
46	6	0	2.790297	-2.170388	0.987013
47	6	0	4.478638	0.984091	0.013423
48	6	0	6.933728	5.065318	-1.045964
49	1	0	6.758813	5.882022	-1.734146
50	6	0	6.024765	4.026045	-0.979233
51	1	0	5.146619	4.038460	-1.615336
52	6	0	5.288274	1.895294	-0.036739
53	6	0	3.702448	-1.155481	0.934665
54	6	0	2.398736	-0.067681	-0.749452
55	6	0	-6.933753	5.065263	1.046014
56	1	0	-6.758864	5.881939	1.734236
57	6	0	8.067225	5.046140	-0.222861
58	6	0	7.368263	2.943384	0.726054
59	1	0	7.529689	2.117614	1.409998
60	6	0	-0.000107	-5.579043	0.000131
61	6	0	-1.062962	-4.646848	-0.633778
62	9	0	-0.568089	-6.367938	0.931045
63	9	0	-2.299284	-5.012924	-0.215408
64	9	0	0.567658	-6.368397	-0.930514
65	9	0	-1.034216	-4.824119	-1.984793

3. Crystal Structure

Single crystals were obtained by purification of column chromatography, followed by recrystallization (CH_2Cl_2/MeOH = 1/1). The X-ray diffraction measurement was carried out at 293 or 173 K. Crystal data of 3a and 3c obtained were listed in Table S5 have been indexed, and are included in the Cambridge Crystallographic Center (CCDC) database with the following numbers: CCDC 1902233 for 3a and 1902234 for 3c. The indexed database contains additional supplementary crystallographic data for this paper and may be accessed without charge at http://www.ccdc.cam.ac.uk/conts/retrieving.html. The CCDC may be contacted by mail at 12 Union Road, Cambridge CB2 1EZ, U.K., by fax at (44) 1223-336-033, or by e-mail at deposit@ccdc.cam.ac.uk.

Table S5. Crystallographic Data

Bistolane	**3a**	**3c**
CCDC #	1902233	1902234
Empirical Formula	$C_{35}H_{14}F_{14}O_2$	$C_{39}H_{22}F_{14}O_2$
Formula Weight	732.46	788.56
Temperature [K]	293(2)	173(2)
Crystal Color / Habit	Yellow / Platelet	Yellow / Platelet
Crystal Size [mm]	0.15 x 0.14 x 0.10	0.16 x 0.15 x 0.09
Crystal System	$P\,2_12_12_1$	$P\,\bar{1}$
Space Group	orthorhombic	triclinic
a [Å]	6.2739(8)	7.6458(4)
b [Å]	20.464(3)	7.7616(3)
c [Å]	23.723(3)	31.5448(10)
α [°]	90	86.116(3)
β [°]	90	83.893(3)
γ [°]	90	66.440(4)
V [Å^3]	3045.8(7)	1705.55(13)
Z	4	2
$R\,[F^2 > 2\sigma(F^2)]$ [a]	0.0816	0.0462
$wR\,(F^2)$ [b]	0.1748	0.1108

[a] $R = \Sigma||F_o| - |F_c|| / \Sigma|F_o|$. [b] $wR = \{[\Sigma w(|F_o| - |F_c|)]/\Sigma w|F_o|\}^{1/2}$.

4. Photophysical Property in CH_2Cl_2 Solution

UV-Vis absorption spectra were recorded using a JASCO V-500 absorption spectrometer. Steady-state photoluminescence (PL) spectra and PL quantum yields were obtained using a Hamamatsu Photonics C11347-01 Absolute PL Quantum Yield Measurement System. Absorption and PL spectra obtained are shown in Figure S21.

(a) **3a**

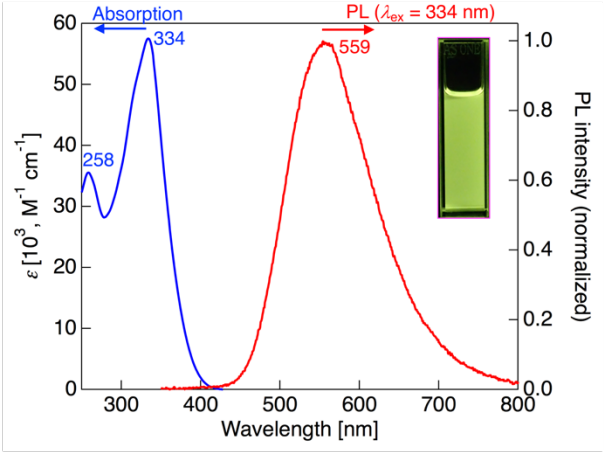

(b) **3b**

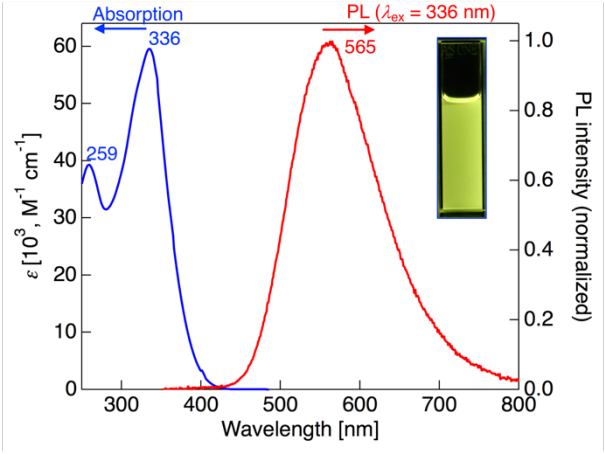

(c) **3c**

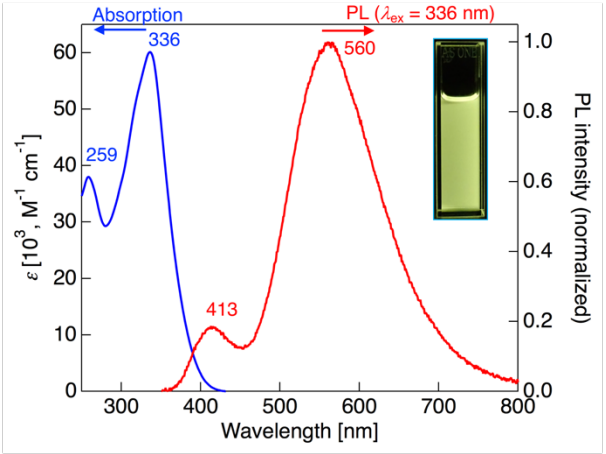

(d) **3d**

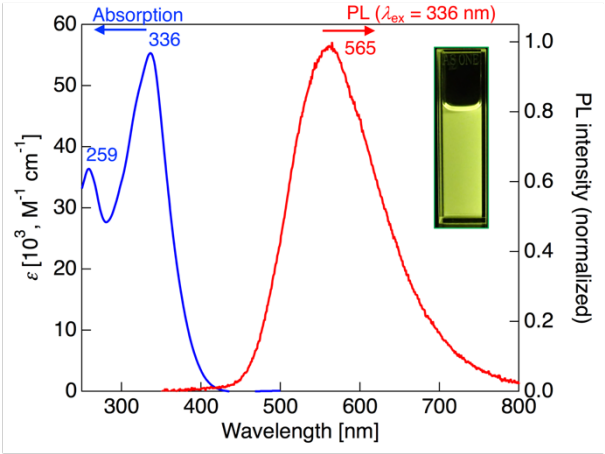

(e) **3e**

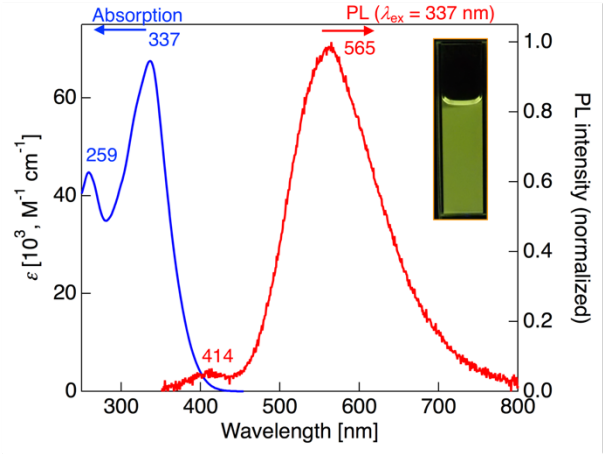

(f) **3f**

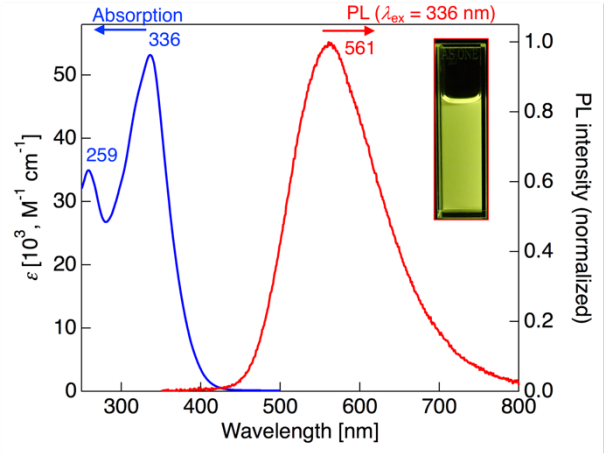

Figure S21. Absorption (blue) and PL spectra (red) of **3a–f** in CH_2Cl_2 solution (concentration: 1.0×10^{-5} M).

5. Photophysical Property in Various Solution

UV-Vis absorption spectra were recorded using a JASCO V-500 absorption spectrometer. Steady-state photoluminescence (PL) spectra and PL quantum yields were obtained using a Hamamatsu Photonics C11347-01 Absolute PL Quantum Yield Measurement System. Absorption and PL spectra obtained are shown in Figure S22.

(a) in Hexane

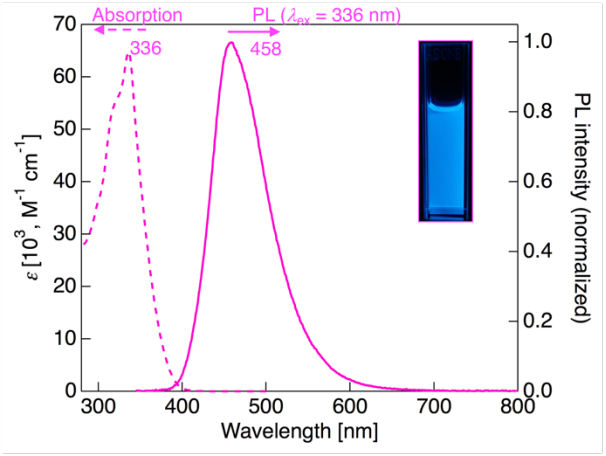

(b) in Toluene

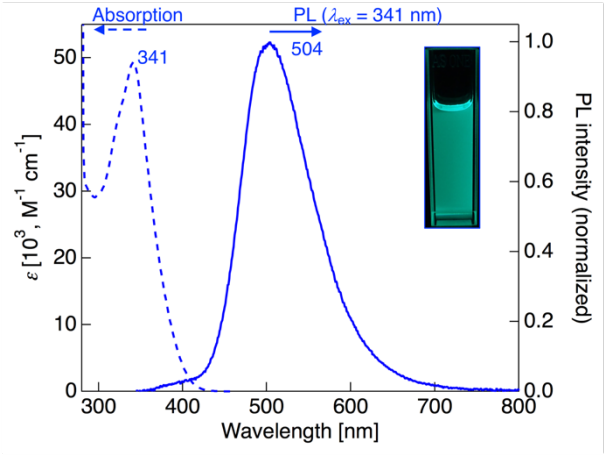

(c) in $CHCl_3$

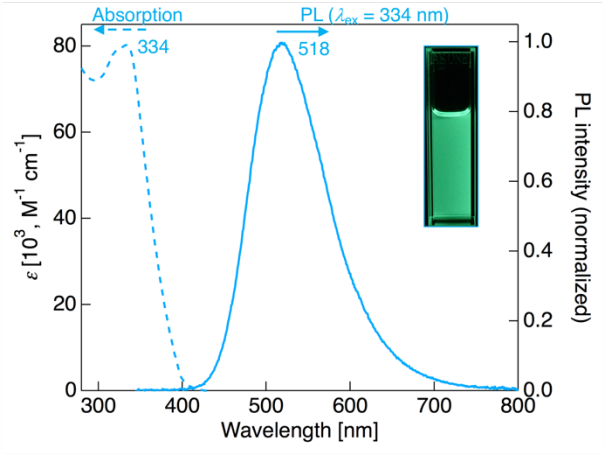

(d) in AcOEt

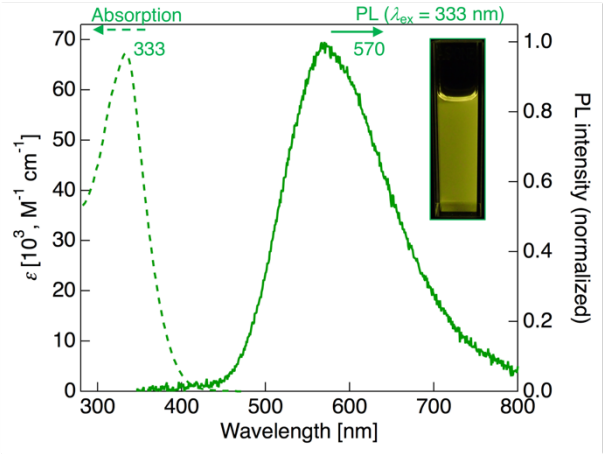

(e) in THF

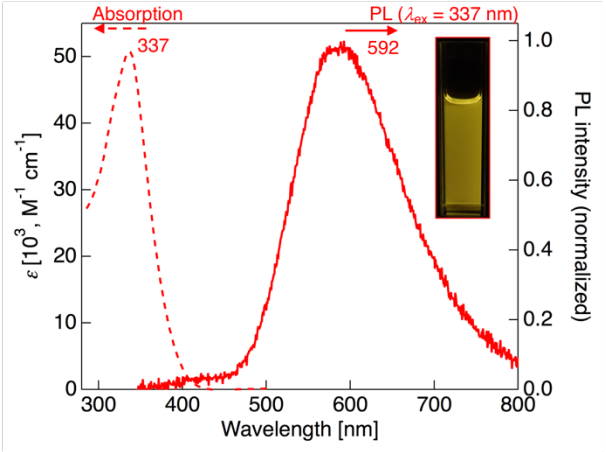

Figure S22. Absorption (dotted line) and PL spectra (solid line) of **3e** in various solution (concentration: 1.0×10^{-5} M).

6. Lippert-Mataga Plot

The Lippert-Mataga plot was constructed by using the relation

$$\nu_{abs}-\nu_{PL} = [2(\mu_e-\mu_g)^2/hca^3]\Delta f + (\nu_{abs}-\nu_{PL})^\circ \qquad \text{(Eq. 1)}$$

where $\nu_{abs}-\nu_{PL}$ is the Stokes' shift, the superscript "°" indicates the absence of solvent, μ_g and μ_e are dipole moments in the ground and the excited states, respectively, D (1D = 1.0x10^{-18} cm$^{5/2}$ g$^{1/2}$ s^{-1}); h is the Planck constant (h = 6.626x10^{-27} erg s); c is the rate of light in vacuum (c = 2.998x10^{-10} cm s^{-1}). a is Onsager cavity radius. The Onsagar radius (a) was estimated by DFT calculation using Gaussian 09 with CAM-B3LYP/6-31G(d) level of theory: a = 6.77 Å for **3e**. The orientation polarizability Δf is defined as

$$\Delta f = [(\varepsilon-1)/(2\varepsilon+1)] - [(n^2-1)/(2n^2+1)] \qquad \text{(Eq. 2)}$$

where ε and n are solvent dielectric constant and refractive index, respectively.

Calculated values for Δf and Stokes shifts ($\nu_{abs}-\nu_{PL}$) for **3e** are summarized in Table S4, and the relationship was shown in Figure S23.

Table S6. Polarizability and Stokes' shift obtained from general solvent effect.

				3e		
	ε	n	Δf	ν_{abs} [cm^{-1}]	ν_{PL} [cm^{-1}]	$\nu_{abs}-\nu_{PL}$ [cm^{-1}]
Hexane	1.88	1.37	–0.0014	29762	21834	7928
Toluene	2.38	1.50	0.014	29326	19841	9485
$CHCl_3$	4.81	1.44	0.149	29940	19305	10635
AcOEt	6.02	1.37	0.200	30030	17544	12486
CH_2Cl_2	8.93	1.42	0.217	29674	17699	11975
THF	7.58	1.41	0.209	29674	16892	12782

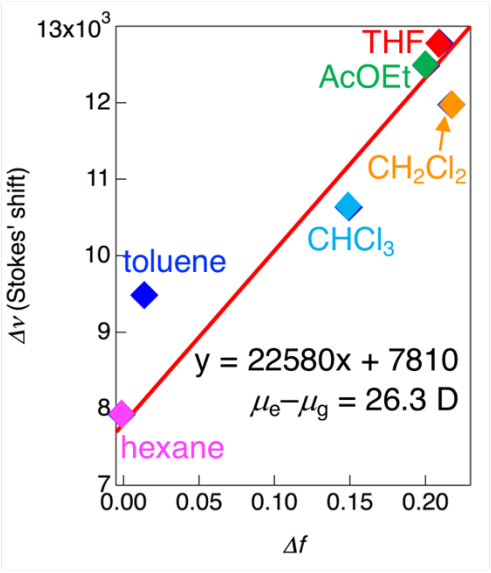

Figure S23. Lippert-Mataga Plot

7. Photophysical Property in Crystal

Excitation spectra, steady-state photoluminescence (PL) spectra, and PL quantum yields were acquired using a Hitachi F-7000 fluorescence spectrometer or a Hamamatsu Photonics C11347-01 Absolute PL Quantum Yield Measurement System. Excitation and PL spectra obtained are shown in Figure S24.

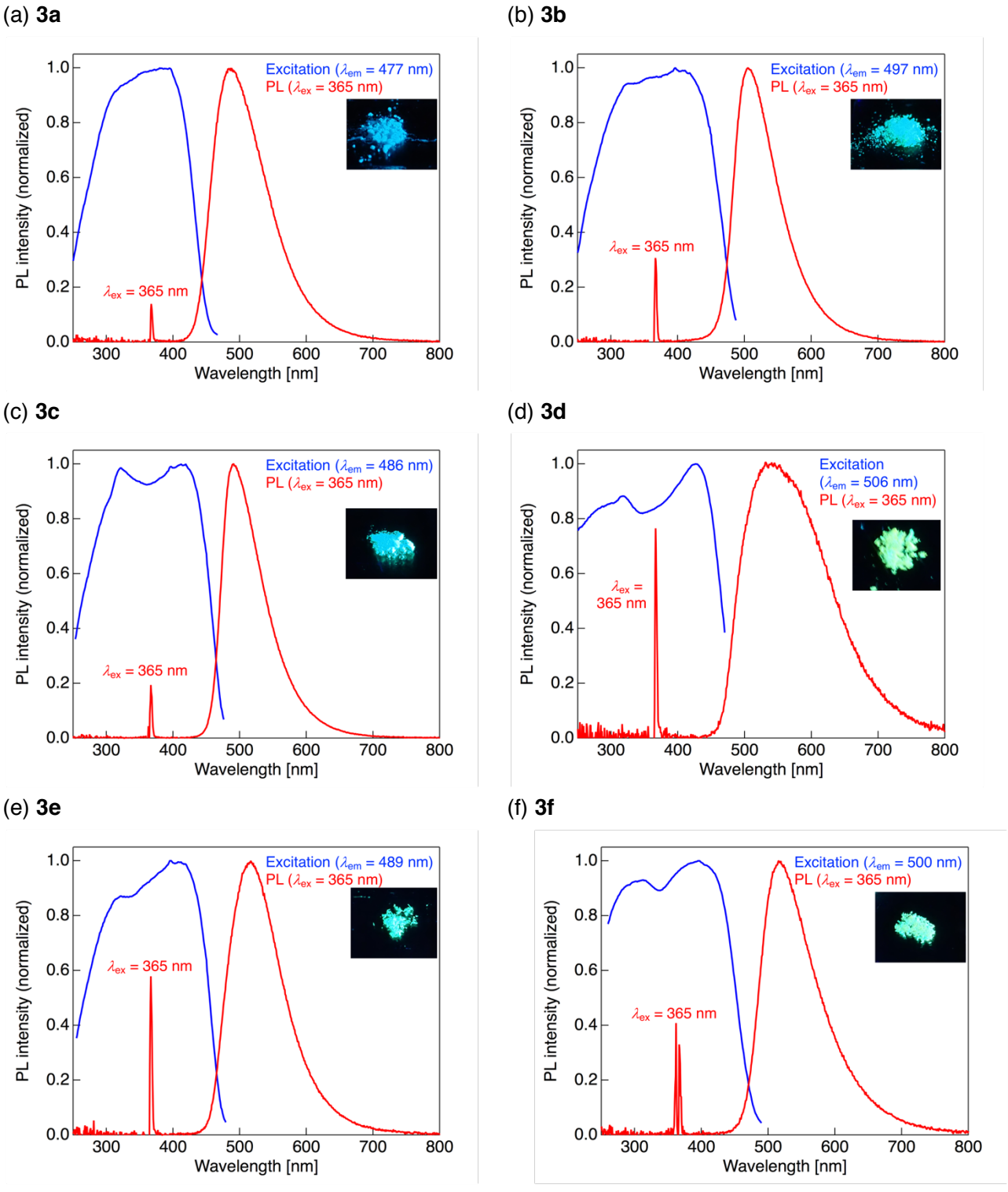

Figure S24. Excitation (blue) and PL spectra (red) of **3a–f** in crystalline state.

8. Transient PL measurement

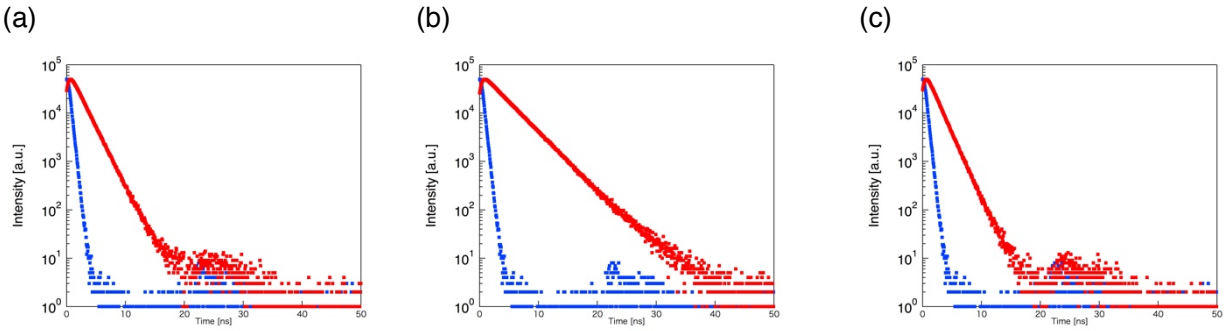

Figure S25. PL decay profiles of **3e** in (a) hexane, (b) CH_2Cl_2, and (c) THF.

Table S7. Photophysical properties of **3e** in various solution.

Solvent	Φ_{PL}	τ [ns]	k_f [10^8, s^{-1}]^a	k_{nr} [10^8, s^{-1}]^a
Hexane	0.71	2.0	3.6	1.5
CH_2Cl_2	0.76	3.6	2.1	0.66
THF	0.21	1.8	1.2	4.5

Φ_{PL}: Quantum yield, τ: PL lifetime, k_f: Fluorescence rate constant, k_{nr}: non-radiative rate constant.
[a]Determined by the following equations: $\Phi_{PL} = k_f/(k_f + k_{nr})$, $\tau = 1/(k_f + k_{nr})$.

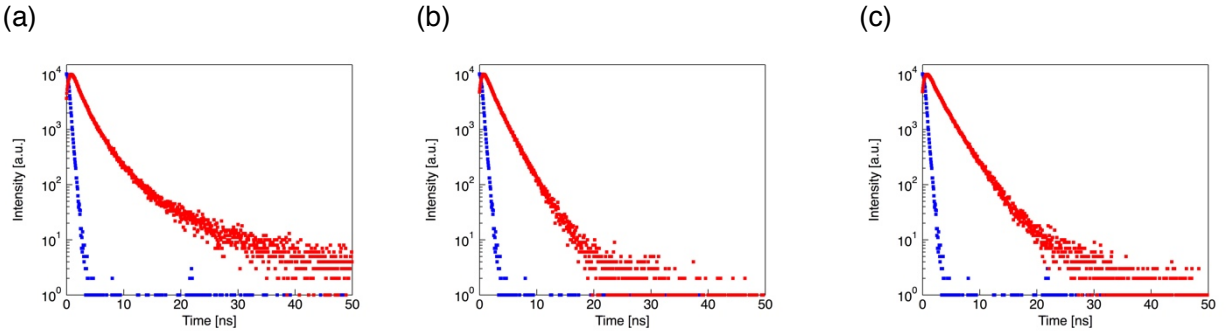

Figure S26. PL decay profiles of (a) **3a**, (b) **3c**, and (c) **3e** in crystal.

Table S8. Photophysical properties of **3a**, **3c**, and **3e** in crystal.

	Φ_{PL}	τ_1 [ns]	τ_2 [ns]	τ_{ave} [ns]	Weight coefficient		k_f [10^8, s^{-1}]^a	k_{nr} [10^8, s^{-1}]^a
					B_1	B_2		
3a	0.43	1.8	6.8	2.4	0.094	0.0039	1.8	2.3
3c	0.55	1.5	2.7	2.0	0.074	0.027	2.8	2.3
3e	0.30	1.9	3.7	2.4	0.080	0.016	1.3	2.9

Φ_{PL}: Quantum yield, τ: PL lifetime, k_f: Fluorescence rate constant, k_{nr}: non-radiative rate constant.
[a]Determined by the following equations: $\Phi_{PL} = k_f/(k_f + k_{nr})$, $\tau = 1/(k_f + k_{nr})$.

9. Powder X-Ray Diffraction Measurement

Powder XRD measurements for **3a–f**, were recorded on a Rigaku RAXIS RAPID II imaging plate area detector using monochromated with Cu$K\alpha$ radiation (λ = 1.5406 Å) by rotating samples along the ϕ-axis and transformed to 2θ–I plot by software. The obtained XRD patterns were shown in Figure S27.

(a) **3a (Simulation)**

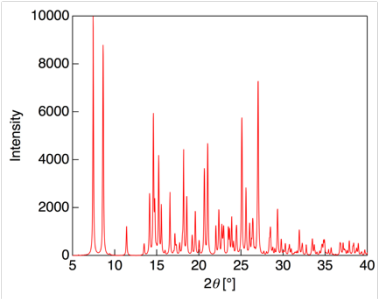

(b) **3c (Simulation)**

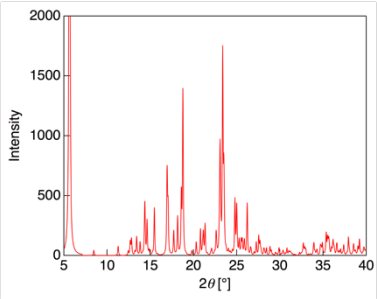

(c) **3a (Experimental)**

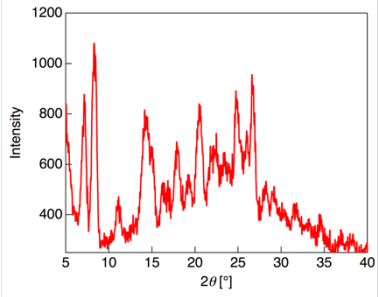

(d) **3c (Experimental)**

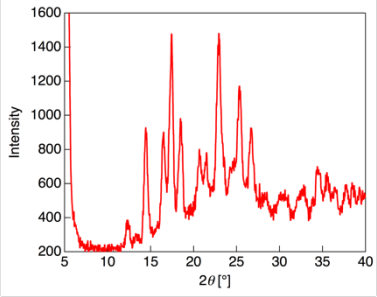

(e) **3b (Experimental)**

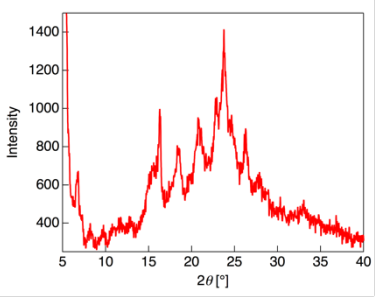

(f) **3d (Experimental)**

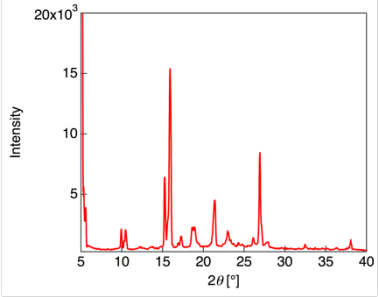

(g) **3e (Experimental)**

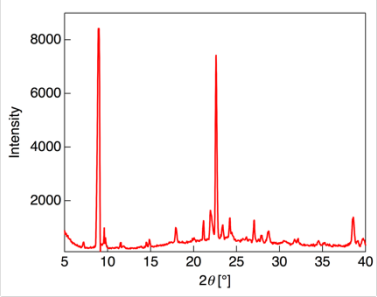

(h) **3f (Experimental)**

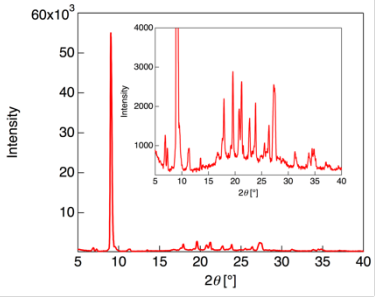

Figure S27. Powder XRD pattern for (a) **3a**, (b) **3c** simulated from single crystal X-ray crystallographic analysis, and (c) **3a**, (d) **3c**, (e) **3b**, (f) **3d**, (g) **3e**, and (h) **3f** obtained experimentally.